Article

Lewis acid promoted aerobic oxidative coupling of thiols with phosphonates by simple nickel(II) catalyst: Substrate scope and mechanistic studies

Jingwen Xue, Miao Zeng, Sicheng Zhang, Zhuqi Chen, and Guochuan Yin

J. Org. Chem., **Just Accepted Manuscript** • DOI: 10.1021/acs.joc.9b00194 • Publication Date (Web): 14 Mar 2019

Lewis acid promoted aerobic oxidative coupling of thiols with phosphonates by simple nickel(II) catalyst: Substrate scope and mechanistic studies

Jing-Wen Xue, Miao Zeng, Sicheng Zhang, Zhuqi Chen, Guochuan Yin*

School of Chemistry and Chemical Engineering, Key laboratory of Material Chemistry for Energy Conversion and Storage (Huazhong University of Science and Technology), Ministry of Education, Hubei Key Laboratory of Material Chemistry and Service Failure, Huazhong University of Science and Technology, Wuhan 430074, PR China.

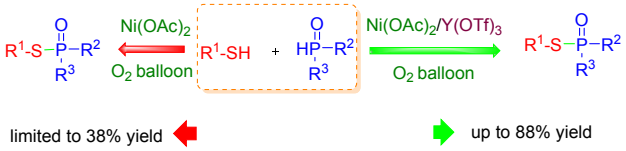

Abstract: Exploring new catalyst for efficient organic synthesis is among the most attractive topics in chemistry. Here, using $Ni(OAc)_2$/LA as catalyst (LA: Lewis acid), a novel catalyst strategy was developed for oxidative coupling of thiols and phosphonates to phosphorothioates with oxygen oxidant. The present studies disclosed that when $Ni(OAc)_2$ alone was employed as the catalyst, the reaction proceeded very sluggishly with low yield, whereas adding non-redox-active metal ions like Y^{3+} to $Ni(OAc)_2$ dramatically promoted its catalytic efficiency. The promotional effect is highly Lewis acidity dependent on the added Lewis acid, and generally, a stronger Lewis acid provided a better promotional effect. The stopped-flow kinetics confirmed that adding $Y(OTf)_3$ can obviously accelerate the activation of thiols by Ni(II), and next accelerate its reaction with phosphonate to generate the phosphorothioate product. ESI-MS characterizations of the catalyst disclosed the formation of the heterobimetallic Ni(II)/Y(III) species in the catalyst solution. Additionally, this Ni(II)/LA catalyst can be applied in synthesis of a series of phosphorothioate compounds including several commercial bioactive compounds. This catalyst

strategy has clearly supported that Lewis acid can significantly improve the catalytic efficiency of these traditional metal ions in organic synthesis, thus opens up new opportunities in their catalyst designs.

1. Introduction

In oxidative coupling reactions, palladium is one of the most popularly employed catalysts because of its highly catalytic activity.[1] In order to improve the catalytic efficiency of the Pd(II) catalyst, Cu(II) was popularly employed as the co-catalyst or oxidant to regenerate the active Pd(II) species from the reduced Pd(0), which was originally inspired from Wacker oxidations.[2-5] In certain cases, organic ligands were also added to the Pd(II) catalyst through ligation to prevent the formation of palladium black in the reaction.[6] However, the drawback is that those organic ligands generally caused the oxidative capability loss of the Pd(II) species because of their electronic donation effect. Recently, it was found that binding Lewis acid (LA) or Brönested acid to the redox metal ions can significantly increase their redox potentials, thus improve their efficiency in oxidations,[7, 8] and several Lewis acid promoted catalysis by redox metal complexes were developed for sulfide oxidation, olefin epoxidation and benzene hydroxylation.[7e, 7f, 8f, 8g] We further found that non-redox metal ions like Sc^{3+} can promote Pd(II)-catalyzed Wacker-type oxidations even much better than Cu^{2+} does, implicating that the Lewis acid properties of Cu^{2+} may have played a significant role in Wacker-type oxidations in addition to its redox properties.[9] Inspired by this finding, a Pd(II)/LA catalyst strategy was defined for organic synthesis, which has been successful in a list of synthesis reactions and biomass transformations.[10] Encouraged by the successes in Pd(II)/LA catalysis, we suspect that this catalyst strategy can be expanded to those organic synthesis catalyzed by other redox metal ions.

Phosphorothioates are well known for their promising bioactivities in pesticides and drugs,[11] and a list of efficient protocols were successfully explored for their synthesis through S-P bond formation.[12, 13] Up to now, in phosphorothioate synthesis through oxidative S-P bond formation, stoichiometric oxidants or hydrogen acceptor were generally employed [12] with only a few exceptions using oxygen/air as oxidant.[13] Therefore, exploring new catalysts which can utilize aerobic oxygen as the oxidant is still highly desirable for this synthesis. The challenge is that thiols could poison the transition metal ions like palladium (II), thereof, direct S-H activation by palladium catalysts were quite rarely reported.[12f, 14] On the other side, although nickel (II) can tolerate the thiols to avoid poisoning, due to its relatively poor activity for oxidative coupling reactions, its applications in the S-H activation reactions were also very limited,[15] and no application for S-P bond formation was reported until now. Inspired by that binding Lewis acid to palladium (II) can significantly improve its catalytic efficiency in organic synthesis,[9, 10] herein, we report the first example of Lewis acid promoted simple Ni(II) catalyst for phosphorothioate synthesis through the oxidative S-P bond formation with oxygen as the terminal oxidant. The new protocol demonstrated here has not only provided an efficient method for phosphorothioate synthesis, but also expanded the Pd(II)/LA catalysis to the cheap metal ions like nickel(II).

Table 1 Optimization of the reaction conditions for the model reaction [a]

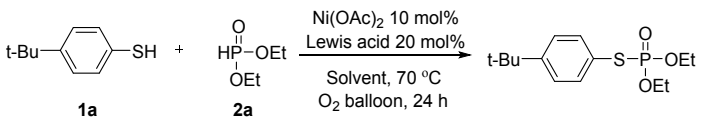

1a **2a**

Entry	Catalyst	Lewis acid	Solvent	Yield (%)[b]
1	$Ni(OAc)_2$	--	DMF	4
2	$Ni(OAc)_2$	NaOTf	DMF	8
3	$Ni(OAc)_2$	$Cu(OTf)_2$	DMF	22
4	$Ni(OAc)_2$	$Zn(OTf)_2$	DMF	30

5	$Ni(OAc)_2$	$Mg(OTf)_2$	DMF	41
6	$Ni(OAc)_2$	$Ca(OTf)_2$	DMF	44
7	$Ni(OAc)_2$	$Al(OTf)_3$	DMF	42
8	$Ni(OAc)_2$	$Sc(OTf)_3$	DMF	58
9	$Ni(OAc)_2$	$Yb(OTf)_3$	DMF	66
10	$Ni(OAc)_2$	$Y(OTf)_3$	DMF	72
11	$Ni(OAc)_2$	$Cu(OAc)_2$	DMF	36
12	$Ni(OAc)_2$	$Y(OTf)_3$	DMA	67
13	$Ni(OAc)_2$	$Y(OTf)_3$	DMSO	39
14	$Ni(OAc)_2$	$Y(OTf)_3$	MeCN	trace
15	$Ni(OAc)_2$	$Y(OTf)_3$	THF	n.d.
16	$Ni(OAc)_2$	$Y(OTf)_3$	CH_3COOH	n.d.

[a] Reaction conditions: **1a** (0.2 mmol), **2a** (0.2 mmol), solvent (2.0 mL), $Ni(OAc)_2$ (10 mol%), Lewis acid (20 mol%), O_2 balloon, 70 °C, 24 h. [b] Isolated yield.

2. Results and discussion

In the initial tests, *p*-tert-butylthiophenol (**1a**) and diethyl phosphite (**2a**) were employed as model substrates for this Ni(II)/LA-catalyzed phosphorothioate synthesis. As shown in Table 1, in the absence of Lewis acid, using 10 mol% $Ni(OAc)_2$ alone with an atmospheric oxygen balloon as the oxidant source, the catalyst showed very sluggish activity, giving only 4% yield of **3a** after 24 h reaction at 70 °C in DMF (Table 1, entry 1). Subsequently, a list of Lewis acids were tested for the $Ni(OAc)_2$ catalyzed model reaction (Table 1, entries 2-11). As shown, adding 20 mol% NaOTf to $Ni(OAc)_2$ slightly improved the yield of **3a** to 8% (Table 1, entry 2). When bivalent metal ions including Cu^{2+}, Zn^{2+}, Mg^{2+} and Ca^{2+} were added to the catalytic system, the catalytic efficiency was improved obviously (Table 1, entries 3-6). For examples, adding $Ca(OTf)_2$ to $Ni(OAc)_2$ provided 44% yield of **3a** (Table 1, entry 5), and adding $Cu(OTf)_2$ as the Lewis acid source also gave 22% yield of **3a**. Remarkably, adding trivalent metal ions such as Al^{3+}, Sc^{3+}, Yb^{3+} and Y^{3+} to $Ni(OAc)_2$ demonstrated much better promotional effects than these of adding bivalent metal ions

(Table 1, entries 7-10). The best result was obtained from adding $Y(OTf)_3$, which provided 72% yield of **3a** (Table 1, entry 10). It is worth mentioning that upon adding the reaction reagents together in DMF solution, the solution turned to black immediately. With the reaction proceeding, it turned back to clear gradually. Further tests confirmed that the color change to black was caused by the reaction of Ni(II)/Y(III) catalyst with **1a** rather than **2a**. In literature, $Cu(OAc)_2$ was popularly proposed to serve as the oxidant in versatile Pd(II)/Cu(II)-catalyzed Wacker-type oxidations and other organic synthesis reactions.[2-5] Here, to specifically address the role of the redox properties of Cu^{2+} cation in this oxidative coupling reaction in the case of using copper(II) salt as a Lewis acid source, $Cu(OAc)_2$ was also tested as the copper(II) source, which provided only 36% yield of **3a** (Table 1, entry 11), much less than these by adding trivalent non-redox metal ions. This result unambiguously supported that the redox properties of Cu^{2+} was not essential for this Ni(II)/LA-catalyzed oxidative coupling reaction. In particular, the promotional effects of added Lewis acids were clearly related with their Lewis acidity, that is, a stronger Lewis acid generally offered a better promotional effect; however, the non-redox Lewis acids alone were in active for this reaction. This is similar to our previous studies with Pd(II)/LA catalysts,[9, 10] and also similar to those Lewis acid promoted stoichiometric and catalytic oxidations with iron and manganese complexes as catalysts.[7d, 7e, 7g 8a-8d] A series of solvents were next investigated for this reaction by adding $Y(OTf)_3$ as the Lewis acid to $Ni(OAc)_2$ catalyst. When DMA and DMSO were employed as solvent, they provided 67% and 39% yields of **3a**, respectively (Table 1, entries 12 and 13). Only trace amount of **3a** were detected with acetonitrile as solvent (Table 1, entry 14), and no **3a** was detected in the case of using tetrahydrofuran or glacial acetic acid as solvent. The influences of solvent on organic synthesis are always very complicated, including affecting the

coordination environment, the potential hydrogen bond network, the redox potentials of the active metal ions, and the stability of the intermediate, etc.[16] The observed influence of solvent effect in present studies could be the mixed apparent effects from different issues which are not fully understood yet. Other parameters such as the ratio of substrate **1a** and **2a**, reaction temperature were also screened, and a ratio of **1a**/**2a** = 1.5/1 was identified as the best substrate molar ratio with 70 °C as an optimal reaction temperature for this reaction (see Table S1 and S2).

Then, the influence of the catalyst loading and the ratio of $Ni(OAc)_2$ and $Y(OTf)_3$ on the efficiency of the model reaction were next evaluated (Table 2). As shown, with 5 mol% $Ni(OAc)_2/Y(OTf)_3$ loading, it gave 62% yield of **3a** (Table 2, entry 1). Having the amount of $Ni(OAc)_2$ at 5 mol% loading with increasing the $Y(OTf)_3$ to 10 mol% made the yield of **3a** improving up to 79% (Table 2, entry 2). Increasing the $Ni(OAc)_2$ loading to 10 mol% with keeping $Y(OTf)_3$ at 5 mol%, 78% yield of **3a** was also obtained (Table 2, entry 3). Notably, the best yield was obtained as 88% by adding 10% loading of $Ni(OAc)_2$ with a 1:1 ratio of $Ni(OAc)_2/Y(OTf)_3$ (Table 2, entry 4). The time course of this reaction also disclosed that adding one equiv. of $Y(OTf)_3$ to the $Ni(OAc)_2$ catalyst could remarkably accelerate the reaction (**Figure 1**), whereas using $Ni(OAc)_2$ alone was very sluggish. Further increasing the loading of $Y(OTf)_3$ caused the yield slightly decrease. For example, using 10% $Ni(OAc)_2$ with 30% $Y(OTf)_3$ loading led the yield decrease to 77% (Table 2, entry 6). It is worth mentioning again that using Lewis acid alone as catalyst is inactive for this reaction (Table 2, entry 7).

Table 2 Ratio and amount of the catalyst loading for the model reaction [a]

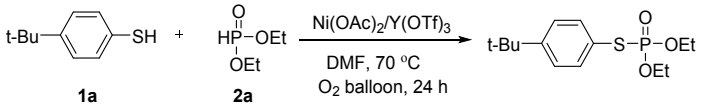

1a 2a

Entry	$Ni(OAc)_2$:$Y(OTf)_3$ (mol%)	Yield (%)[b]
1	5:5	62
2	5:10	79
3	10:5	78
4	10:10	88
5	10:20	86
6	10:30	77
7	0:10	ND

[a] Reaction conditions: **1a** (0.3 mmol), **2a** (0.2 mmol), DMF (2.0 mL), $Ni(OAc)_2$ (5-10 mol%), $Y(OTf)_3$ (5-30 mol%), O_2 balloon, 70 °C, 24 h. [b] Isolated yield.

Next, a series of control experiments were conducted under the optimal conditions to identify the role of added $Y(OTf)_3$ in this reaction (Table 3). When the reaction was catalyzed by $Ni(OAc)_2$ alone, only 20% yield of **3a** was obtained under the standard conditions (Table 3, entry 1), which was much less than that by adding $Y(OTf)_3$ to $Ni(OAc)_2$ (88%, Table 3, entry 6 as the standard conditions). Using $Y(OTf)_3$ alone as a catalyst did not show any catalytic activity for this reaction (Table 3, entry 2). These two experiments clearly supported that the added Lewis acid did promote the Ni(II)-catalyzed oxidative coupling of thiol and phosphonate to phosphorothioate. In order to distinguish the roles of OTf^- anion and Y^{3+} cation from added $Y(OTf)_3$ in this reaction, three controlled experiments were designed by using $Ni(OAc)_2$/HOTf, $Ni(OTf)_2$, and $Ni(OTf)_2$/$Y(OTf)_3$ as catalyst independently (Table 3, entries 3-5). As shown, adding 30 mol% loading of HOTf , which provides the identical amount of OTf^- anion to that of 10 mol% $Y(OTf)_3$), to $Ni(OAc)_2$ as the catalyst provided only 9% yield of the **3a** product. In addition, it is worth mentioning that adding HOTf even suppressed the catalytic efficiency of $Ni(OAc)_2$ (Table 3, 9% vs 20%, entries 1 vs 3). Subsequently, using $Ni(OTf)_2$ as catalyst provided 14% yield of **3a** (Table 3, entry 4), and combining $Ni(OTf)_2$ and $Y(OTf)_3$) together as the catalyst also offered only

29 % yield of **3a** (Table 3, entry 5), much less than that of using $Ni(OAc)_2/Y(OTf)_3$, thus excluding the anion exchange between $Ni(OAc)_2$ and $Y(OTf)_3$ to generate $Ni(OTf)_2$ as the active catalyst for this reaction. In order to address the role of OTf^- in the reaction, two parallel experiments were performed by using YCl_3 and $Y(OAc)_3$ to replace $Y(OTf)_3$ for $Ni(OAc)_2$-catalyze model reaction, and 67% and 40% yield of **3a** were obtained, respectively (Table 3, entries 7 and 8). In a specific experiment using $Zn(BF_4)_2$ to replace $Zn(OTf)_2$ in the Ni(II)/Zn(II) catalyst, it also provided 27% yield of **3a**, comparing to 30% yield with that of adding $Zn(OTf)_2$ (Table 3, entry 9 vs 10). Taken together, these results clearly supported that the Y^{3+} cation promoted the Ni(II)-catalyzed oxidative coupling reaction, and the counter anion of Y^{3+} affected the promotional effect through affecting the Lewis acidity of Y^{3+}. Remarkably, the OAc^- anion is essential for this reaction as well as those in previous Pd(II)/LA catalysis.[9, 10]

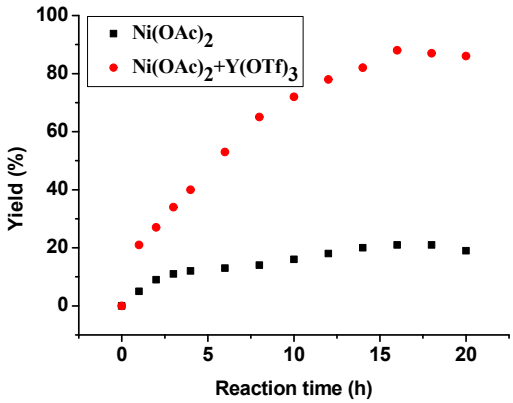

Figure 1 The time course of $Ni(OAc)_2/Y(OTf)_3$ catalyzed oxidative S-P bond formation for phosphorothioate synthesis. Reaction conditions: *p*-tert-butylthiophenol (0.3 mmol), diethyl phosphite (0.2 mmol), $Ni(OAc)_2$ (10 mol%), $Y(OTf)_3$ (10 mol%), DMF (2.0 mL), 70 °C.

Under the standard conditions, the substrate scope of thiophenols/aliphatic thiols and phosphates to synthesize the thiophosphate products was examined. As summarized in **Scheme 1**, aromatic thiols **1** having different *ortho* and *para* electron-donating groups like CH_3 or CH_3O were coupled readily with diethyl phosphonate to generate the desired products in good yields (**3b-3d**,

78-82%).When aromatic thiols bearing an electron-withdrawing groups (F, Cl, Br or NO_2) were employed, the corresponding products were also obtained in satisfactory yields (**3e-3i**, 70-86%). The substrates having functional groups like amine and hydroxyl could also react with diethyl phosphonate smoothly, giving the corresponding thiophosphate products in 40% and 75% yields, respectively (**3j** and **3k**). To our delight, both naphthalene-1-thiol and naphthalene-2-thiol were also compatible for this Ni(II)/Y(III)-catalyzed S-P bond formation reaction, offering the desired products in 86% and 76% yields, respectively (**3l** and **3m**). When the thiophenols were replaced with benzylthiophenol, this Ni(II)/Y(III)-catalyzed oxidative S-P bond formation also proceeded efficiently with diethyl phosphonate (**3n** and **3o**).

Table 3 Control experiments for the model reaction [a]

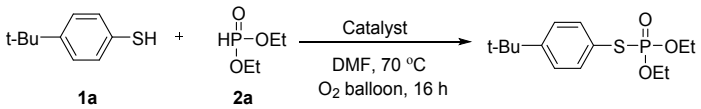

1a **2a**

Entry	Catalyst	Yield (%)[b]
1	$Ni(OAc)_2$	20
2	$Y(OTf)_3$	ND
3	$Ni(OAc)_2$+HOTf (30 mol%)	9
4	$Ni(OTf)_2$	14
5	$Ni(OTf)_2$+$Y(OTf)_3$	29
6	$Ni(OAc)_2$+$Y(OTf)_3$	88
7	$Ni(OAc)_2$+YCl_3	67
8	$Ni(OAc)_2$+$Y(OAc)_3$	40
9[c]	$Ni(OAc)_2$+$Zn(BF_4)_2$	27

10[d]	$Ni(OAc)_2$+$Zn(OTf)_2$	30

[a] Reaction conditions: **1a** (0.3 mmol), **2a** (0.2 mmol), DMF (2.0 mL), $Ni(OAc)_2$ (10 mol%), $Y(OTf)_3$ (10 mol%), O_2 balloon, 70 °C, 16 h. [b] Isolated yield. [c] $Zn(BF_4)_2$ (10 mol%) used as the Lewis acid. [d] $Zn(OTf)_2$ (10 mol%) used as the Lewis acid.

Furthermore, aliphatic thiols also reacted well with diethyl phosphonate under the current conditions (**3p-3v**). Cyclohexanethiol was coupled readily with diethyl phosphonate to give the coupling product **3p** in 72% yield. Aliphatic thiols such as octane-1-thiol, butane-1-thiol, *iso*-butane-1-thiol, pentane-1-thiol, and ester functionalized chain aliphatic thiols were all tolerated with this Ni(II)/Y(III) catalyst, giving 63-77% yields (**3q-3v**), respectively. Aside from diethyl phosphonate, other phosphates such as diisopropyl and dibutyl phosphonate could also be coupled with *p*-tert-butylthiophenol smoothly to give the corresponding products **3w** and **3x** in good yields. In addition to dialkyl phosphates, diphenyl phosphine oxide and ethyl phenylphosphinate were also tested as substrate to couple with *p*-tert-butylthiophenol, which gave 65% and 75% yields of the corresponding products (**3y** and **3z**), respectively. Notably, in the control experiments using $Ni(OAc)_2$ alone as catalyst, the yields of the corresponding coupling products were much lower than that obtained by Ni(III)/Y(III) catalyst (see the data in the parentheses in **Scheme 1**). These data clearly highlights the crucial role of the added Lewis acid in promoting the catalytic efficiency of Ni(II) in this oxidative coupling reaction, as well as those in Pd(II)/LA catalysis.[9, 10]

In order to illustrate the practical applications of this Ni(II)/LA catalyst in phosphorothioate synthesis, we applied this protocol in the synthesis of several commercial bioactive compounds as shown in **Scheme 2**. Iprobenfos **3aa**, a pesticide with excellent control effects on rice leaf blast and ear mites,[17] could be readily synthesized through the oxidative coupling of diisopropyl

phosphonate and benzyl thiol with $Ni(OAc)_2/Y(OTf)_3$ catalyst in 62% yield. Similarly, inezin **3ab**, which has both preventive and therapeutic effects on rice diseases such as rice blast, stalk and rice sclerotium,[18] could also be afforded with 65% yield under the standard conditions. Demeton **3ac**, mainly used to prevent and cure sucker pests such as aphids and spider mites on cotton and fruit trees,[19] was also synthesized by this protocol with 72% yield. It is worth mentioning that, due to the highly reactive of the ethylthiolyl group in **5** to organic oxidant in its oxidative synthesis, there were only a few reports on the synthesis of **3ac**.[12d, 12e] Finally, echothiopate, a drug that can be used for the treatment of glaucoma with a long-lasting effect,[20] could be easily synthesized from **6** through a two-step reaction, including oxidative coupling through this protocol to **3ad** followed by salinization with iodomethane,[20b] giving 69% and 85% of yields in two steps, respectively. Again, the activity of $Ni(OAc)_2$ alone in these synthesis was always much lower than these of $Ni(OAc)_2/Y(OTf)_3$ catalyst as demonstrated in the parentheses of **Scheme 2**, thus highlighting the super activity of Ni(II)/LA catalyst as well as those of Pd(II)/LA catalysts.[9, 10]

Scheme 1 Substrate scope of Ni(II)/Y(III)-catalyzed oxidative coupling reactions [a].

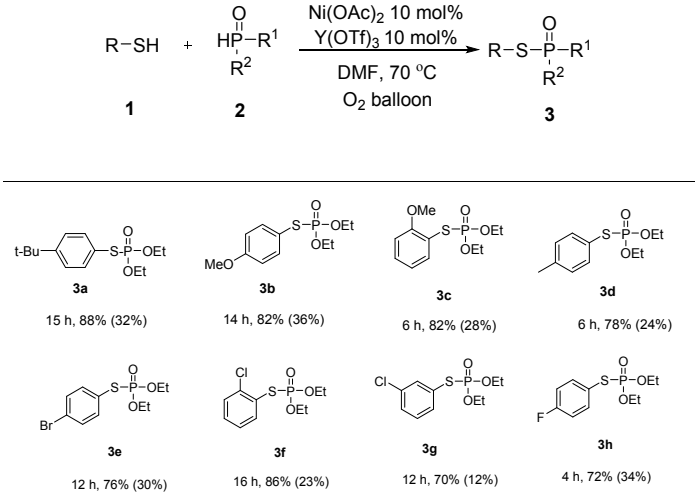

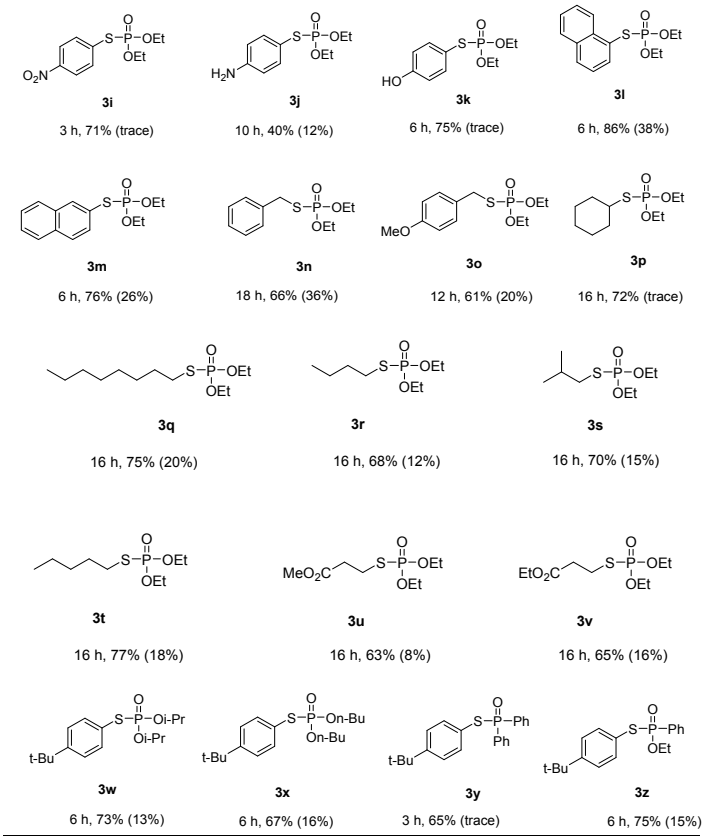

[a] Standard conditions: 1 (0.3 mmol), 2 (0.2 mmol), DMF (2.0 mL), $Ni(OAc)_2$ (10 mol%), $Y(OTf)_3$ (10 mol%), O_2 balloon, 70 °C. [b] Isolated yield. The values in parentheses were obtained with only $Ni(OAc)_2$ as catalyst.

Scheme 2 Illustrated pesticide and drug synthesis by Ni(II)/Y(III) catalyst.

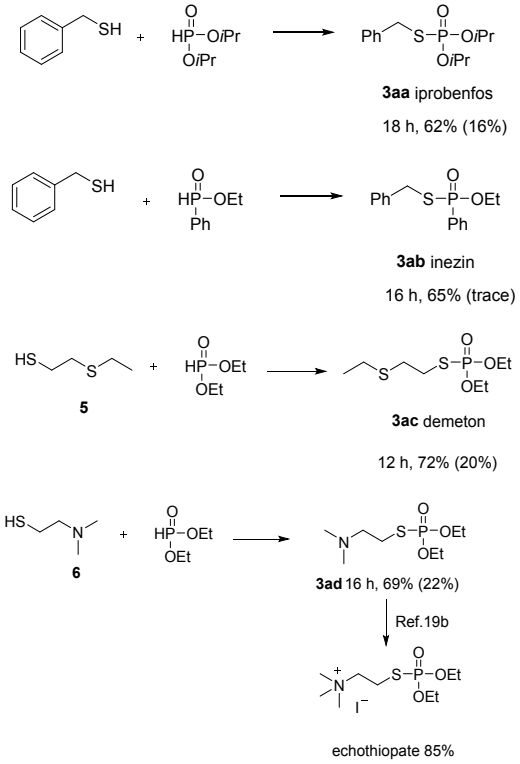

To gain insights into the mechanism of this $Ni(OAc)_2/Y(OTf)_3$-catalyzed oxidative coupling reaction, mechanistic studies were next conducted by performing a list of control experiments (**Scheme 3**). In literature, it has been proposed that all of S-centered radical,[12d, 12e, 13a] P-centered radical,[12d, 12e, 13a] and disulfide [12e, 12g, 13a] could serve as the intermediates in oxidative S-P bond formation under certain conditions, and the existences of the radical intermediates were evidenced by radical scavengers or trapped by olefin.[12g] Here, adding radical scavengers including 2,2,6,6-tetramethyl-1-piperidinyloxy (TEMPO) and 2,6-di-tertbutyl-4-methylphenol (BHT) did not quench the oxidative coupling between **1a** and **2a** under the standard conditions, which still gave **3a** in good yields (68% and 63%) (**Scheme 3**, eq. 1). In addition, the radical trapping experiments by adding styrene to **1a** or **2a** under standard conditions also did not yield any radical adduct as product (**Scheme 3**, eqs. 2 and 3). Therefore, these results clearly supported that the free radical mechanism was not involved in this oxidative coupling reaction, and no P-centered radicals or S-centered radicals was involved in phosphorothioate formation in present studies. Next, in the absence of **2a**, treating **1a** under the standard conditions for 6 h led to the formation of the disulfide **4a** in 90% yield, whereas treating **2a** itself did not lead the corresponding homo-coupling product formation (**Scheme 3**, eqs. 4 and 5). This information implicated that the disulfide 4a may exist in the reaction mixture and function as an intermediate in phosphorothioate formation as well as those in literature.[12e, 12g, 13a]

Scheme 3 Experiments for mechanistic studies.

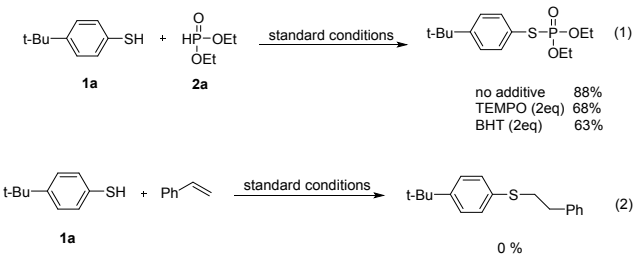

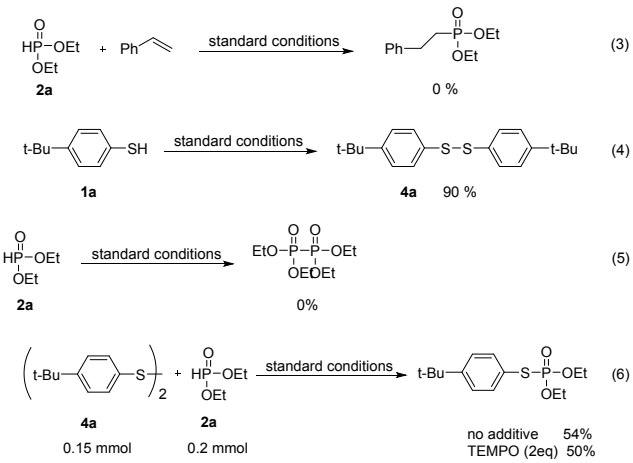

Standard conditions: DMF (2.0 mL), $Ni(OAc)_2$ (10 mol%), $Y(OTf)_3$ (10 mol%), O_2 balloon, 70 °C, 16 h.

In addition, it was reported that S-centered radical served as an intermediate for the phosphorothioate formation under certain conditions.[12d, 12e, 13a] Consequently, this Ni(II)/Y(III)-catalyzed oxidative coupling reaction between **4a** and **2a** was conducted under the standard conditions, and it did provide **3a** in 54% yield. However, adding TEMPO only demonstrated ignorable influence on this coupling, which still gave 50% yield (**Scheme 3**, eq. 6). Apparently, the S-centered radical did not exist in the system to serve as the intermediate for **3a** formation. It is worth mentioning that, the reaction of **1a** with **2a** under the standard conditions caused the solution turning to black immediately, whereas the solution color for **4a** reacting with **2a** changed to black much slower, indicating that they were two different reaction processes. Now, these experiments also raise a new query, that is, whether **4a** is an intermediate for the S-P bond formation, since **4a** may have chance to occur in the reaction medium as disclosed by Eq. 4. To address this issue, the kinetic studies to compare the reactivity between **4a** and **1a** in their reactions with **2a** were conducted paralleling under the standard conditions (**Fig. S1**). As displayed, in the whole time course, the yields of phosphorothioate product from **4a** were always much lower than that of using **1a** as substrate, even in the case of adding identical equivalent of **4a** in place of **1a**. If **4a** were the intermediate for the phosphorothioate formation from **1a** and **2a**, the

yield of phosphorothioate should be always not lower, even higher than that by using **1a** as substrate in the whole time course. Taken together, these experiments supported that **4a** was not on the pathway of **1a** reacting with **2a** to phosphorothioate. However, **4a** may be generated in the reaction mixture, and can be transferred to **3a** under the standard conditions, that is, formation of **4a** from **1a** is reversible.

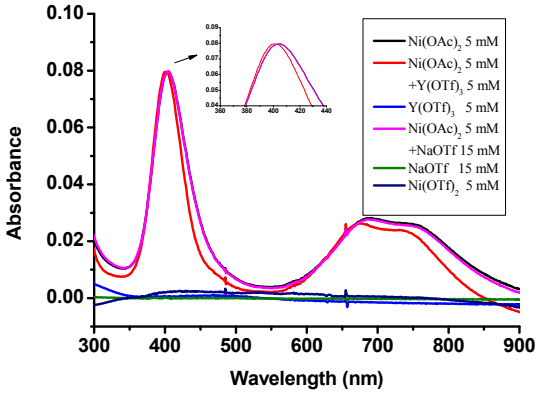

Figure 2 UV-Vis spectra of $Ni(OTf)_2$, $Ni(OAc)_2$ and $Y(OTf)_3$, NaOTf with their mixture in DMF at room temperature.

In order to address the active species and the reaction details for the oxidative S-P bond formation by $Ni(OAc)_2/Y(OTf)_3$ catalyst, a series of UV-Vis studies were conducted with the DMF solution of $Ni(OAc)_2/Y(OTf)_3$. As shown in **Figure 2**, $Ni(OAc)_2$ alone in DMF demonstrated two distinct absorbance bands which can be attributed to the metal-ligand-charge-transfer (MLCT) transition having maximum band around 405 nm (ε = 16 M^{-1} cm^{-1}) and d-d transition having a broad band around 680-760 nm (ε = 5.6 M^{-1} cm^{-1}), respectively. Adding one equiv. of $Y(OTf)_3$ to $Ni(OAc)_2$ in DMF caused a minor but non-ignorable blue-shift of the d-d transition band, however, it did not change the shape of the band, implicating a slight coordination environment change of the Ni(II) species, for example, a plausibly slight d-d gap increase, caused by adding $Y(OTf)_3$. Similarly, a much weaker, but also

non-ignorable blue-shift of the MLCT band was also observed for the same solution as well. To eliminate the possibility of the absorbance band migration caused by the OTf^- anion exchange, the UV-Vis measurements were also conducted by using three equiv. of NaOTf to replace one equiv. of $Y(OTf)_3$ in the solution; unsurprisingly, no absorbance band migration was observed as shown in **Figure 2**. Unexpectedly, $Ni(OTf)_2$ in DMF demonstrated a flat curve with no obvious MLCT and d-d transition band. These results clearly supported that the OTf^- anion exchange can be excluded to generate $Ni(OTf)_2$ from $Ni(OAc)_2/Y(OTf)_3$, at least, to a significant level, since adding $Y(OTf)_3$ to $Ni(OAc)_2$ in DMF did not weaken its absorbance, whereas $Ni(OTf)_2$ has no obvious band in this area.

As well as the phenomena observed from above oxidative coupling reactions, that is, adding **1a** to the catalyst solution containing $Ni(OAc)_2/Y(OTf)_3$ led to the immediate color change to black, here, the UV-Vis spectrum also disclosed the formation a new species having the absorbance band occurring around 490 nm, and simultaneously, the original d-d transition band of the Ni(II) decayed (**Figure S3**). In the stoichiometric treatment of **1a** with $Ni(OAc)_2/Y(OTf)_3$ in DMF solution, along with the concentration of **1a** increasing, the absorbance intensity of the new band increased as well (**Figure S3**). In the controlling experiment using $Ni(OAc)_2$ alone, a similar new band was also observed immediately when treating it with **1a**. However, compared with the new band generated by treating **1a** with $Ni(OAc)_2$, the band from **1a** with $Ni(OAc)_2/Y(OTf)_3$ demonstrated a slightly blue-shift as well as the influence of $Y(OTf)_3$ to $Ni(OAc)_2$ in DMF solution (**Figure 2** vs **3**). This new band can be rationally assigned to the absorbance of the RS-Ni(II) or RS-Ni(II)/Y(III) intermediate by the reaction of **1a** with $Ni(OAc)_2$ or $Ni(OAc)_2/Y(OTf)_3$, respectively, in which the presence of the Y^{3+} made the absorbance slightly

blue-shifted. Following the general procedures reported for kinetic studies in literature,[21] the stopped-flow kinetics for the formation of this intermediate disclosed that the presence of $Y(OTf)_3$ accelerated its formation rate, giving the k_2 values of 3.14×10^{-3} mM^{-1} s^{-1} for $Ni(OAc)_2/Y(OTf)_3$ and 4.15×10^{-4} mM^{-1} s^{-1} for $Ni(OAc)_2$ alone, respectively (**Figure 4**). Remarkably, the stability of this intermediate was significantly improved by the presence of $Y(OTf)_3$ (**Figure S7**). That is, the presence of $Y(OTf)_3$ made the formation of the RS-Ni(II)/Y(III) intermediate faster than that of the corresponding RS-Ni(II) intermediate, meanwhile it also stabilized the RS-Ni(II)/Y(III) intermediate to make its decay slower than that of the corresponding RS-Ni(II) intermediate.

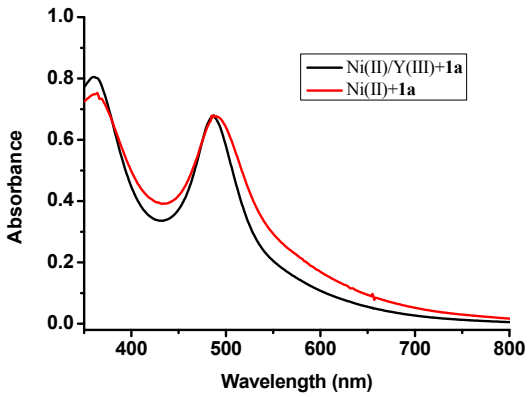

Figure 3 UV-Vis spectra of $Ni(OAc)_2$ with **1a** in the presence (black) and absence (red) of $Y(OTf)_3$ from kinetic process tested by the stopped-flow instrument. [Catalyst] = 1 mM, [**1a**] = 1 mM, solvent: DMF, room temperature.

In the similar treatment of **2a** with the catalytic solution, there was no color change observed and the UV-Vis spectrum also remained no change, indicating that in the oxidative coupling S-P formation with $Ni(OAc)_2/Y(OTf)_3$ catalyst, the catalyst first reacted with **1a** which consequently reacted with **2a** to generate the product. Consequently, the reaction kinetics of **2a** with the *in-situ* generated RS-Ni(II) or RS-Ni(II)/Y(III) intermediate was investigated with the stopped-flow instrument. As displayed in **Figure 5**, the presence of $Y(OTf)_3$ accelerated the reaction of this intermediate with **2a**, making the **2a** dependent decay faster than that of in the

absence of $Y(OTf)_3$, that is, the slope of the concentration dependence is larger for the catalysts system with $Y(OTf)_3$, giving k_2 values of 3.32×10^{-5} mM^{-1} s^{-1} for $Ni(OAc)_2/Y(OTf)_3$ and 1.62×10^{-5} mM^{-1} s^{-1} for $Ni(OAc)_2$ alone, respectively (Figure 5). It is worth mentioning that, there exists two pathways for the decay of both RS-Ni(II) and RS-Ni(II)/Y(III) intermediates; one is to generate disulfide as mentioned earlier (eq. 4, *vide supra*), the other is to react with **2a** to generate the target phosphorothioate products (if **2a** were added). Therefore, the k_{obs} in Figure 5 is not the real k_{obs} for the phosphorothioate formation, but the total decaying k_{obs} for both disulfide and phosphorothioate formations. The larger slope of the concentration dependence for the reaction between the RS-Ni(II)/Y(III) intermediate and **2a** than that of the RS-Ni(II) intermediate and **2a** in Figure 5 indicated that the reaction between **2a** and RS-Ni(II)/Y(III) intermediate is faster than that of the RS-Ni(II) intermediate with **2a** (k_2 value of 3.32×10^{-5} vs 1.62×10^{-5} mM^{-1} s^{-1}), thus $Y(OTf)_3$ accelerates the second step of the reaction. Taken together, these kinetic data clearly confirmed that adding $Y(OTf)_3$ to $Ni(OAc)_2$ accelerated its reaction with **1a**, and next also accelerated it further reaction with **2a** to the corresponding phosphorothioate product.

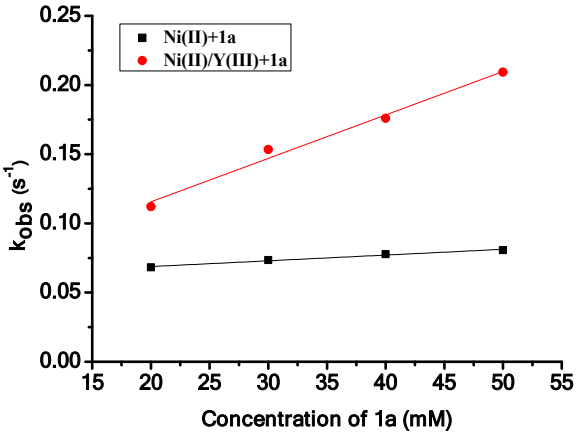

Figure 4 Correlation of substrate concentration with the k_{obs} constant for the formation of RS-Ni(II) or RS-Ni(II)/Y(III) intermediates by the reaction of $Ni(OAc)_2$ with **1a** in the absence (black) and presence (red) of $Y(OTf)_3$.

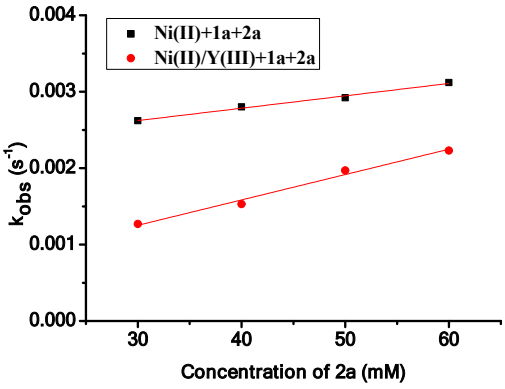

Figure 5 Correlation of substrate concentration with the k_{obs} constant for the disappearance of the RS-Ni(II)/Y(III) or RS-Ni(II) intermediate when their reacting with **2a**.

In clarifying the reactivity between the disulfide compound **4a** and the Ni(II)/Y(III) catalyst, it was found that the color of the reaction solution turned black gradually in 10 minutes at 70 °C, which was much slower than that of reaction with **1a**. In the UV-Vis tests at room temperature, the characteristic bands of the Ni(II) species remained unchanged after adding **4a** to the DMF solution of the Ni(II)/Y(III) catalyst (**Figure S4**), and no new band was observed for the corresponding RS-Ni(II)/Y(III) species as that from the reaction of **1a** with the Ni(II)/Y(III) catalyst. These results supported that thiophenol **1a** is more feasibly activated by Ni(II)/Y(III) catalyst than the disulfide compound **4a**. Taken together, although **4a** can react with **2a** to generate the corresponding phosphorothioate product under the catalytic conditions, the UV-Vis studies disclosed that its kinetic behaves was different from that of **1a** reacting with Ni(II)/Y(III) catalyst. Thus, **4a** may be generated from **1a** under the catalytic conditions as displayed by Eq. 4, and can be further transformed to the corresponding phosphorothioate product as shown in Eq. 6; however, it is not on the pathway of **1a** reacting with **2a** to the phosphorothioate product.

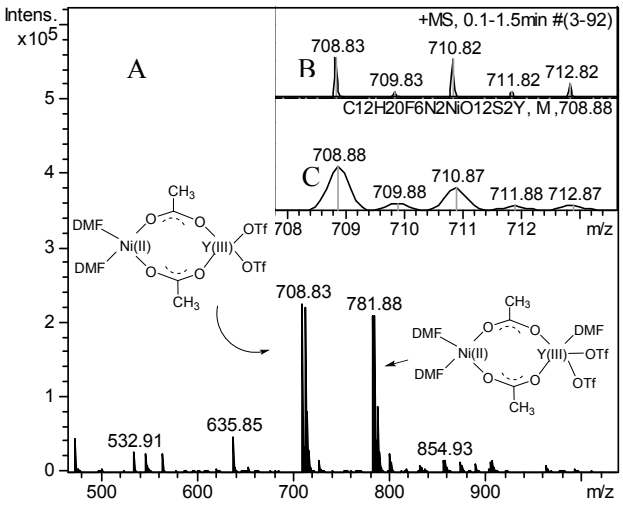

Figure 6 ESI-MS spectrum with plausible structures of (a) $Ni(OAc)_2/Y(OTf)_3$ in DMF at 70 °C for 20 minutes. (b) Ni(II)/Y(III) dimeric structure at m/z = 708.83, and (c) its theoretical isotopic peak distribution.

In previous studies, the heterobimetallic structures were was even proposed for the Pd(II)/LA catalyzed organic synthesis based on NMR and UV-Vis characterizations, in which two acetate bridge linked the Pd(II) and LA together,[9, 10] and similar heterobimetallic palladium(II) complexes were isolated with X-ray characterizations in literature.[22] Here, as implicated from the synthetic results and UV-Vis studies, a new nickel (II) species may have been *in-situ* generated in the catalytic solution of $Ni(OAc)_2/Y(OTf)_3$, and is responsible for the improved catalysis. Indeed, the electrospray ionization mass spectrometry (ESI-MS) analysis of above catalytic solution disclosed a major mass peak at m/z=708.83 (Figure 6). Based on the similarly crucial role of acetate in both Pd(II)/LA and Ni(II)/Y(III) catalysis, the structure of this mass peak could be assigned to the acetate bridged heterobimetallic Ni(II)/Y(II) structure as well as those in Pd(II)/LA catalysts. This mass spectrum agreed well with the theoretical prediction of the corresponding isotopic peak distribution patterns, thus provided valuable evidence to support the existence of a heterobimetallic Ni(II)/Y(III) species in the catalytic solution. In addition to the mass peak at m/z=708.83, another peak at m/z=781.88 can be assigned to the Ni(II)/Y(III) dimeric structure

with one more DMF ligated, and also agreed well with the theoretical prediction of the corresponding isotopic peak distribution patterns. Due to the paramagnetic properties of the Ni(II) cation, the NMR characterizations of the Ni(II)/Y(III) species were not accessible.

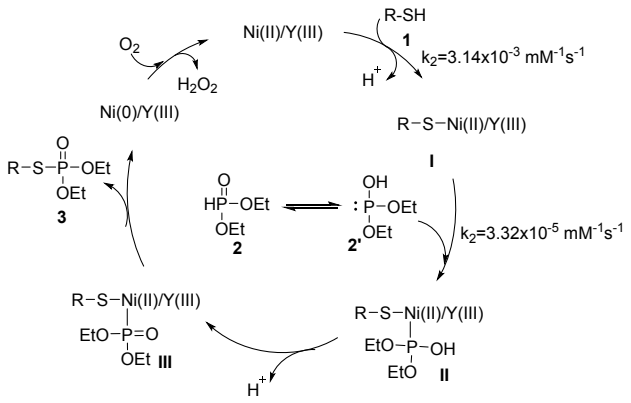

Scheme 4 A plausible mechanism for Ni(II)/Y(III) catalyzed oxidative coupling S-P formation reaction to phosphorothioate (R: p-tert-butylphenyl).

According to above studies with the reported mechanisms in literatures,[12f, 12g] a simplified mechanism was proposed for this Ni(II)/Y(III)-catalyzed oxidative coupling reaction as shown in **Scheme 4**. In this mechanism, a heterometallic Ni(II)/Y(III) species (abbreviated as Ni(II)/Y(III)) was *in-situ* generated in the catalytic solution, which served as the activity species for the oxidative coupling reaction. Initially, the Ni(II)/Y(III) species activated the S-H bond of thiophenol **1** to generate the RS-Ni(II)/Y(III) intermediate **I**. Subsequently, the ligation of **2'** (the tautomerization structure of **2** [12g, 13a]) to the intermediate **I** generated the intermediate **II** which gave the intermediate **III** via proton release. Next, the reductive elimination of the intermediate **III** to produce the final product **3** with Ni(0)/Y(III) complex. Finally, the Ni(0)/Y(III) species was oxidized by oxygen to regenerate the active Ni(II)/Y(III) species to achieve the catalytic cycle as well as those in other Ni(II)-catalyzed synthesis.[23] In the whole catalytic cycle, the formation of the heterobimetallic Ni(II)/Y(III) species accelerated the formation of the intermediate **I**, and next

accelerated its reaction with **2'**, thus improving the catalytic efficiency. In addition, through HPLC analysis of H_2O_2 generation, it was found that adding $Y(OTf)_3$ to $Ni(OAc)_2$ substantially increased the H_2O_2 formation in the catalytic solution (**Figure S12**). Since detecting the Ni(0) and Ni(0)/Y(III) species was not successful in the catalytic solution, the direct evidence to confirm the presence of Lewis acid accelerating the aerobic oxidation of Ni(0) was not available. However, the increased H_2O_2 formation may have implicated that the presence of Lewis acid also accelerated the oxidation of Ni(0) back to the active Ni(II)/Y(III) species.

3. Conclusion

The present work illustrated a novel Ni(II)/LA catalyst strategy for the oxidative coupling of thiols and phosphonates to phosphorothioates. The presence of certain non-redox metal ions as Lewis acid could significantly improve the catalytic efficiency of the simple nickel (II) salt, and the promotional effect was highly the Lewis acidity dependent on the added Lewis acid. That is, a stronger Lewis acid provided a better promotional effect. The kinetic studies also disclosed that the presence of $Y(OTf)_3$ could obviously accelerate the activation of thiol by Ni(II) to generate the RS-Ni(II)/Y(III) intermediate, and further accelerate the next oxidative coupling with phosphonate to generate the corresponding phosphorothioate product. ESI-MS characterizations of the $Ni(OAc)_2/Y(OTf)_3$ in DMF solvent disclosed the formation of a heterobimetallic Ni(II)/Y(III) species which is responsible for the improved catalysis. This Ni(II)/Y(III) catalyst also demonstrated a wide substrate scope for the S-P formation through oxidative coupling, and was successfully exampled in several commercial bioactive compound synthesis. The present Ni(II)/Y(III) catalyst not only demonstrated its applications in phosphorothioate synthesis through

oxidative coupling, but also convinced that the Pd(II)/LA catalysis can be expanded to other redox metal ions, which opens up new opportunity for the catalyst design in versatile organic synthesis.

4. Experimental Section

4.1 Materials and analytical methods

Unless otherwise noted, all reagents were purchased from commercial suppliers and used without further purification. Compound **5** and **6** were synthesized following the literatures with modifications.[24] UV-Vis spectra were collected on Agilent Technologies Cary-8454 UV-Vis spectrometer. UV-Vis kinetic analyses were performed on the Stopped-Flow Reaction Analyzer-SX20 (Applied Photophysics). The reactions were monitored by TLC with Haiyang GF-254 silica gel plates (Qingdao Haiyang chemical industry Co. Ltd, Qingdao, China) using UV light or $KMnO_4$ as visualizing agents as needed. Flash column chromatography was performed using 200-300 mesh silica gel at increased pressure. ^1H NMR spectra and ^{13}C NMR spectra were respectively recorded on Brüker AV-400 spectrometers. Chemical shifts (δ) were expressed in ppm with TMS as the internal standard, and coupling constants (*J*) were reported in Hz. High-resolution mass spectra were obtained on mass spectrometer by using ESI FT-ICR Mass.

4.2 General procedure for the synthesis of 5 (2-(ethylthio)ethane-1-thiol).

A mixture of 2-(ethylthio)ethan-1-ol (20 mmol) and thiourea (20 mmol) in 48% aq. HBr (4.25 mL) was refluxed overnight under argon. Then the reaction was cooled down to room temperature. Next, concentrated aq. NaOH (1.6 g, 40 mmol) was added carefully, and the resulting mixture was refluxed overnight under Ar. After that, the reaction solution was cooled down to room temperature, neutralized with concentrated HCl, and extracted with CH_2Cl_2 (100 mL). The

organic phase was separated, washed with water, dried over Na_2SO_4, and evaporated to give **5** as colorless oil, which was used without further purification (1.98 g, 81% yield).

4.3 General procedure for the synthesis of 6 (2-(dimethylamino)ethane-1-thiol).

A 100 mL round bottom flask was dried, degassed, and refilled with argon. Then, dimethylamine (10 mL, 2 M solution in THF) was added in and next solidified into the white solid in a liquid nitrogen bath. Then the liquid nitrogen bath was replaced by an ice bath, ethylene sulfide (1.3 eq., 26 mmol) in 20 mL THF was added into above dimethylamine solution dropwise. The reaction solution was next stirred for 2 hours at 0 °C under nitrogen. Finally, the solution was concentrated via rotary evaporation at 40 °C to yield the corresponding product **6** as a colorless liquid (1.47 g, 70% yield).

4.4 General procedure for oxidative coupling reaction with $Ni(OAc)_2$/$Y(OTf)_3$ catalyst in DMF

In a typical procedure, $Ni(OAc)_2$ (3.5 mg, 0.02 mmol) and $Y(OTf)_3$ (10.7 mg, 0.02 mmol) were dissolved in DMF (2 mL) in a glass tube. After pre-stirring the prepared solution for 20 min under 70 °C, **1** (0.3 mmol) and **2** (0.2 mmol) were added in. The glass tube was next connected with an O_2 balloon, and stirred at 70 °C for desired reaction time. After the reaction, 5 mL H_2O was added into the reaction mixture, which was next extracted by ethyl acetate (3 × 10 mL) for three times. The combined organic phase was dried over anhydrous Na_2SO_4, and next the solvent was removed under reduced pressure. The crude products were purified by column chromatography on a silica gel (petroleum ether/EtOAc: 1/1–5/1) to give the desired products. Control experiments were carried out carefully, and the results are summarized in **Table 1** and **Table 3**.

4.5 General procedure for UV-Vis experiments in DMF

In a typical UV-Vis experiment to characterize the catalyst, $Ni(OAc)_2$ (5 mmol) and $Y(OTf)_3$ (5 mmol) were dissolved in DMF in a glass tube, which was pre-stirred for 20 min under 70 °C, then cooled down to room temperature for UV-Vis studies. The UV-Vis scans were carried out by using $Ni(OAc)_2$ (5 mmol), $Ni(OTf)_2$ (5 mmol), $Y(OTf)_3$ (5 mmol) and $Ni(OAc)_2$ /$Y(OTf)_3$ (5 mmol) in DMF at room temperature independently.

4.6 General procedure for the stopped-flow experiments in DMF

(a) In a typical kinetic experiment to determine the formation rate of the RS-Ni(II) or RS-Ni(II)/Y(III) species, 1 mM Ni(II) or Ni(II)/Y(III) catalyst with excess of **1a** (20, 30, 40, and 50 mM) were dissolved in DMF separately, then, the *in-situ* generation kinetics of the RS-Ni(II) or RS-Ni(II)/Y(III) species was monitored at 490 nm with the stopped-flow instrument by detecting their reaction at room temperature. The k_{obs} constants for the formation of the RS-Ni(II) or RS-Ni(II)/Y(III) species were calculated according to the first-order reaction, and the k_2 value was calculated from a set of the k_{obs} constants with different **1a** concentrations, including 20, 30, 40, and 50 mM.

(b) To investigate the reaction kinetics of **2a** with the RS-Ni(II) or RS-Ni(II)/Y(III) species, 1 mM Ni(II) or Ni(II)/Y(III) catalyst were dissolved in DMF as one sample, and 1 mM **1a** with excessive **2a** (30, 40, 50, and 60 mM) were dissolved in DMF in another sample. The decay of the *in-situ* generated RS-Ni(II) or RS-Ni(II)/Y(III) species was monitored with the stopped-flow instrument at 490 nm through the *in-situ* reaction of two samples at room temperature. The k_{obs} constants for the decay of the RS-Ni(II) or RS-Ni(II)/Y(III) species were calculated according to the first-order reaction, and the k_2 value was calculated from a set of the k_{obs} constants with the different **2a** concentrations, including 30, 40, 50, and 60 mM.

S-(4-(tert-butyl)phenyl) O,O-diethyl phosphorothioate ***(3a)*** [12f] Colorless oil (53.2 mg, 88% yield); ^{1}H NMR (400 MHz, $CDCl_3$) δ 7.48 (d, *J* = 6.7 Hz, 2H), 7.36 (d, *J* = 8.3 Hz, 2H), 4.31-4.05 (m, 4H), 1.32 (m, 15H). $^{13}C\{^{1}H\}$ NMR (101 MHz, $CDCl_3$) δ 152.4 (d, *J* = 3.1 Hz), 134.3 (d, *J* = 5.1 Hz), 126.5 (d, *J* = 2.1 Hz), 122.8 (d, *J* = 7.2 Hz), 64.0 (d, *J* = 6.1 Hz), 34.7), 31.2, 16.0 (d, *J* = 7.2 Hz). ^{31}P NMR (162 MHz, $CDCl_3$) δ 23.4.

O,O-diethyl S-(4-methoxyphenyl) phosphorothioate ***(3b)*** [12f, 13b] colorless oil (45.3 mg, 82% yield); ^{1}H NMR (400 MHz, $CDCl_3$) δ 7.47 (d, *J* = 6.8 Hz, 2H), 6.88 (d, *J* = 8.6 Hz, 2H), 4.30-4.07 (m, 4H), 3.80 (s, 3H), 1.31 (t, *J* = 7.0 Hz, 6H). $^{13}C\{^{1}H\}$ NMR (101 MHz, $CDCl_3$) δ 160.5 (d, *J* = 2.8 Hz), 136.3 (d, *J* = 4.7 Hz), 116.6 (d, *J* = 7.3 Hz), 115.0 (d, *J* = 2.4 Hz), 63.9 (d, *J* = 6.3 Hz), 55.4, 16.0 (d, *J* = 7.1 Hz).

O,O-diethyl S-(2-methoxyphenyl) phosphorothioate ***(3c)*** [13b] colorless oil (45.5 mg, 82% yield); ^{1}H NMR (400 MHz, $CDCl_3$) δ 7.60 (d, *J* = 7.6 Hz, 1H), 7.35 (t, *J* = 7.8 Hz, 1H), 6.93 (dd, *J* = 14.4, 7.8 Hz, 2H), 4.22 (dq, *J* = 14.3, 7.1 Hz, 4H), 3.88 (s, 3H), 1.31 (t, *J* = 7.0 Hz, 6H). $^{13}C\{^{1}H\}$ NMR (101 MHz, $CDCl_3$) δ 159.5 (d, *J* = 5.0 Hz), 136.9 (d, *J* = 4.4 Hz), 130.9 (d, *J* = 2.8 Hz), 121.3 (d, *J* = 2.3 Hz), 114.5 (d, *J* = 7.0 Hz), 111.5 (d, *J* = 2.2 Hz), 63.8 (d, *J* = 5.8 Hz), 55.9, 16.0 (d, *J* = 7.5 Hz).

O,O-diethyl S-(p-tolyl) phosphorothioate ***(3d)*** [12f, 13b] colorless oil (40.6 mg, 78% yield); ^{1}H NMR (400 MHz, $CDCl_3$) δ 7.44 (d, *J* = 6.8 Hz, 2H), 7.15 (d, *J* = 7.7 Hz, 2H), 4.29-4.08 (m, 4H), 2.34 (s, 3H), 1.31 (t, *J* = 7.0 Hz, 6H). $^{13}C\{^{1}H\}$ NMR (101 MHz, $CDCl_3$) δ 139.3 (d, *J* = 3.0 Hz), 134.6 (d, *J* = 5.1 Hz), 130.2 (d, *J* = 2.3 Hz), 122.8 (d, *J* = 7.3 Hz), 64.08 (d, *J* = 6.2 Hz), 21.2, 16.0 (d, *J* = 7.2 Hz).

S-(4-bromophenyl) O,O-diethyl phosphorothioate ***(3e)*** [13b] colorless oil (49.4 mg, 76% yield); ^{1}H NMR (400 MHz, $CDCl_3$) δ 7.46 (dd, *J* = 18.5, 7.9 Hz, 4H), 4.20 (dt, *J* = 12.6, 8.3 Hz, 4H), 1.32 (t, *J* = 7.0 Hz, 6H). $^{13}C\{^1H\}$ NMR (101 MHz, $CDCl_3$) δ 136.0 (d, *J* = 5.2 Hz), 132.5 (d, *J* = 2.1 Hz), 125.9 (d, *J* = 7.2 Hz), 123.6 (d, *J* = 3.5 Hz), 64.3 (d, *J* = 6.4 Hz), 16.0 (d, *J* = 7.1 Hz).

S-(2-chlorophenyl) O,O-diethyl phosphorothioate ***(3f)*** [13b] colorless oil (48.3 mg, 86% yield); ^{1}H NMR (400 MHz, $CDCl_3$) δ 7.76 (d, *J* = 7.4 Hz, 1H), 7.46 (d, *J* = 7.6 Hz, 1H), 7.35-7.21 (m, 2H), 4.33-4.14 (m, 4H), 1.32 (t, *J* = 7.0 Hz, 6H). $^{13}C\{^1H\}$ NMR (101 MHz, $CDCl_3$) δ 137.9 (d, *J* = 6.9 Hz), 136.8 (d, *J* = 4.0 Hz), 130.3 (dd, *J* = 5.7, 2.4 Hz), 127.5 (d, *J* = 2.3 Hz), 126.4 (d, *J* = 6.9 Hz), 64.4 (d, *J* = 6.3 Hz), 16.0 (d, *J* = 7.3 Hz).

S-(3-chlorophenyl) O,O-diethyl phosphorothioate ***(3g)*** [13b] colorless oil (39.3 mg, 70% yield); ^{1}H NMR (400 MHz, $CDCl_3$) δ 7.49 (s, 1H), 7.39 (d, *J* = 7.4 Hz, 1H), 7.23 (dt, *J* = 15.6, 7.9 Hz, 2H), 4.23-4.04 (m, 4H), 1.25 (t, *J* = 7.0 Hz, 6H). $^{13}C\{^1H\}$ NMR (101 MHz, $CDCl_3$) δ 134.8 (d, *J* = 2.3 Hz), 134.1 (d, *J* = 5.4 Hz), 132.5 (d, *J* = 5.3 Hz), 130.3 (d, *J* = 2.0 Hz), 129.2 (d, *J* = 2.6 Hz), 128.5 (d, *J* = 7.1 Hz), 64.3 (d, *J* = 6.3 Hz), 16.0 (d, *J* = 7.1 Hz).

O,O-diethyl S-(4-fluorophenyl) phosphorothioate ***(3h)*** [12f, 13b] colorless oil (38 mg, 72% yield); ^{1}H NMR (400 MHz, $CDCl_3$) δ 7.63-7.48 (m, 2H), 7.05 (t, *J* = 8.5 Hz, 2H), 4.28-4.10 (m, 4H), 1.32 (t, *J* = 7.0 Hz, 6H). $^{13}C\{^1H\}$ NMR (101 MHz, $CDCl_3$) δ 164.6 (d, *J* = 3.3 Hz), 162.1, 136.7 (dd, *J* = 8.4, 5.0 Hz), 121.7 (d, *J* = 3.7 Hz), 116.6 (dd, *J* = 22.1, 2.2 Hz), 77.4, 77.1, 76.8, 64.2 (d, *J* = 6.4 Hz), 16.0 (d, *J* = 7.1 Hz).

O,O-diethyl S-(4-nitrophenyl) phosphorothioate ***(3i)*** [12f, 13b] colorless oil (41.4 mg, 71% yield); ^{1}H NMR (400 MHz, $CDCl_3$) δ 8.20 (d, *J* = 8.5 Hz, 2H), 7.77 (d, *J* = 7.4 Hz, 2H), 4.36-4.13 (m, 4H),

1.35 (t, J = 7.0 Hz, 6H). $^{13}C\{^{1}H\}$ NMR (101 MHz, $CDCl_3$) δ 147.8, 136.3 (d, J = 6.6 Hz), 134.1 (d, J = 6.0 Hz), 124.1, 64.7 (d, J = 6.5 Hz), 16.0 (d, J = 7.0 Hz).

S-(4-aminophenyl) O,O-diethyl phosphorothioate ***(3j)*** [12f, 13b] pale yellow oil (21 mg, 40% yield); ^{1}H NMR (400 MHz, $CDCl_3$) δ 7.24 (d, J = 6.7 Hz, 2H), 6.55 (d, J = 8.2 Hz, 2H), 4.18-4.01 (m, 4H), 3.72 (s, 2H), 1.24 (t, J = 7.0 Hz, 6H). $^{13}C\{^{1}H\}$ NMR (101 MHz, $CDCl_3$) δ 146.7 (d, J = 2.6 Hz), 135.3 (d, J = 4.6 Hz), 114.7 (d, J = 2.4 Hz), 111.9, 62.9 (d, J = 6.3 Hz), 15.0 (d, J = 7.2 Hz).

O,O-diethyl S-(4-hydroxyphenyl) phosphorothioate ***(3k)*** [12f, 13b] colorless oil (39.2 mg, 75% yield); ^{1}H NMR (400 MHz, $CDCl_3$) δ 8.59 (s, 1H), 7.22 (dd, J = 8.5, 2.0 Hz, 2H), 6.56 (d, J = 8.2 Hz, 2H), 4.21-4.03 (m, 4H), 1.27 (t, J = 7.0 Hz, 6H). $^{13}C\{^{1}H\}$ NMR (101 MHz, $CDCl_3$) δ 157.6 (d, J = 3.1 Hz), 135.7 (d, J = 4.7 Hz), 116.1 (d, J = 2.4 Hz), 112.2 (d, J = 7.2 Hz), 63.6 (d, J = 6.8 Hz), 15.0 (d, J = 7.0 Hz).

O,O-diethyl S-(naphthalen-1-yl) phosphorothioate ***(3l)*** [12f] colorless oil (51 mg, 86% yield); ^{1}H NMR (400 MHz, $CDCl_3$) δ 8.53 (d, J = 8.4 Hz, 1H), 7.97-7.78 (m, 3H), 7.60 (t, J = 7.4 Hz, 1H), 7.52 (t, J = 7.4 Hz, 1H), 7.45 (t, J = 7.7 Hz, 1H), 4.21-4.02 (m, 4H), 1.18 (t, J = 7.0 Hz, 6H). $^{13}C\{^{1}H\}$ NMR (101 MHz, $CDCl_3$) δ 135.3 (d, J = 5.6 Hz), 134.7 (d, J = 4.1 Hz), 134.3 (d, J = 2.2 Hz), 130.3 (d, J = 3.4 Hz), 128.6, 127.1, 126.5, 125.9, 125.7 (d, J = 3.4 Hz), 123.8 (d, J = 8.1 Hz), 64.2 (d, J = 6.6 Hz), 16.0 (d, J = 7.1 Hz).

O,O-diethyl S-(naphthalen-2-yl) phosphorothioate ***(3m)*** [13b] colorless oil (45 mg, 76% yield); ^{1}H NMR (400 MHz, $CDCl_3$) δ 8.08 (s, 1H), 7.80 (dd, J = 8.4, 5.1 Hz, 3H), 7.61 (d, J = 8.5 Hz, 1H), 7.50 (dd, J = 6.1, 3.2 Hz, 2H), 4.30-4.12 (m, 4H), 1.30 (t, J = 7.0 Hz, 6H). $^{13}C\{^{1}H\}$ NMR (101 MHz, $CDCl_3$) δ 134.4 (d, J = 6.8 Hz), 133.6 (d, J = 2.2 Hz), 133.1 (d, J = 1.9 Hz), 130.9 (d, J =

4.1 Hz), 129.0, 127.7 (d, *J* = 3.2 Hz), 127.1, 126.8, 123.8 (d, *J* = 7.4 Hz), 64.2 (d, *J* = 6.3 Hz), 16.1 (d, *J* = 7.1 Hz).

S-benzyl O,O-diethyl phosphorothioate ***(3n)*** [13b] colorless oil (34.4 mg, 66% yield); ^{1}H NMR (400 MHz, $CDCl_3$) δ 7.41-7.22 (m, 5H), 4.19-3.94 (m, 6H), 1.28 (t, *J* = 7.0 Hz, 6H). $^{13}C\{^{1}H\}$ NMR (101 MHz, $CDCl_3$) δ 137.5 (d, *J* = 5.4 Hz), 128.9, 128.7, 127.6, 63.5 (d, *J* = 5.7 Hz), 35.0 (d, *J* = 3.9 Hz), 16.0 (d, *J* = 7.4 Hz).

O,O-diethyl S-(4-methoxybenzyl) phosphorothioate ***(3o)*** [13b] colorless oil (35.4 mg, 61% yield); ^{1}H NMR (400 MHz, $CDCl_3$) δ 7.28 (d, *J* = 8.4 Hz, 2H), 6.85 (d, *J* = 8.5 Hz, 2H), 4.19-3.95 (m, 6H), 3.80 (s, 3H), 1.30 (t, *J* = 7.0 Hz, 6H). $^{13}C\{^{1}H\}$ NMR (101 MHz, $CDCl_3$) δ 159.1, 130.1, 129.5 (d, *J* = 5.7 Hz), 114.0, 63.5 (d, *J* = 5.8 Hz), 55.3, 34.6 (d, *J* = 3.8 Hz), 16.0 (d, *J* = 7.3 Hz).

S-cyclohexyl O,O-diethyl phosphorothioate ***(3p)*** [12f, 13b] colorless oil (36.3 mg, 72% yield); ^{1}H NMR (400 MHz, $CDCl_3$) δ 4.16 (dt, *J* = 15.5, 8.6 Hz, 4H), 3.28 (dd, *J* = 21.6, 10.5 Hz, 1H), 2.08 (d, *J* = 9.9 Hz, 2H), 1.78-1.71 (m, 2H), 1.63-1.46 (m, 3H), 1.45-1.24 (m, 9H). $^{13}C\{^{1}H\}$ NMR (101 MHz, $CDCl_3$) δ 63.4 (d, *J* = 6.1 Hz), 45.6 (d, *J* = 3.5 Hz), 35.3 (d, *J* = 6.0 Hz), 25.9, 25.3, 16.1 (d, *J* = 7.3 Hz).

O,O-diethyl S-octyl phosphorothioate ***(3q)*** [12f, 13b] colorless oil (42.4 mg, 75% yield); ^{1}H NMR (400 MHz, $CDCl_3$) δ 4.34-4.07 (m, 4H), 2.90-2.74 (m, 2H), 1.68 (dt, *J* = 14.9, 7.4 Hz, 2H), 1.34 (dd, *J* = 25.8, 18.7 Hz, 16H), 0.88 (t, *J* = 6.5 Hz, 3H). $^{13}C\{^{1}H\}$ NMR (101 MHz, $CDCl_3$) δ 63.4 (d, *J* = 5.9 Hz), 31.8, 30.9 (dd, *J* = 14.5, 4.9 Hz), 29.0 (d, *J* = 13.2 Hz), 28.6, 22.6, 16.1 (d, *J* = 7.3 Hz), 14.1.

S-butyl O,O-diethyl phosphorothioate ***(3r)*** [13b] colorless oil (30.8 mg, 68% yield); ^{1}H NMR (400 MHz, $CDCl_3$) δ 4.32-4.04 (m, 4H), 2.84 (dt, *J* = 14.5, 7.4 Hz, 2H), 1.74-1.61 (m, 2H), 1.40 (dt, *J* =

27.1, 7.1 Hz, 8H), 0.93 (t, *J* = 7.3 Hz, 3H). $^{13}C\{^{1}H\}$ NMR (101 MHz, $CDCl_3$) δ 63.4 (d, *J* = 5.9 Hz), 32.8 (d, *J* = 5.8 Hz), 30.6 (d, *J* = 3.9 Hz), 21.7, 16.1 (d, *J* = 7.3 Hz), 13.5.

O,O-diethyl S-isobutyl phosphorothioate ***(3s)*** [13b] colorless oil (31.7 mg, 70% yield); ^{1}H NMR (400 MHz, $CDCl_3$) δ 4.31-4.03 (m, 4H), 2.74 (dd, *J* = 13.1, 6.8 Hz, 2H), 1.91 (dt, *J* = 13.2, 6.7 Hz, 1H), 1.37 (t, *J* = 7.0 Hz, 6H), 1.01 (d, *J* = 6.6 Hz, 6H). $^{13}C\{^{1}H\}$ NMR (101 MHz, $CDCl_3$) δ 63.4 (d, *J* = 5.9 Hz), 39.4 (d, *J* = 3.9 Hz), 29.5 (d, *J* = 6.0 Hz), 21.6, 16.1 (d, *J* = 7.3 Hz).

O,O-diethyl S-pentyl phosphorothioate ***(3t)*** colorless oil (37 mg, 77% yield); ^{1}H NMR (400 MHz, $CDCl_3$) δ 4.27 – 4.07 (m, 4H), 2.83 (dt, *J* = 14.5, 7.4 Hz, 2H), 1.68 (dd, *J* = 14.5, 7.3 Hz, 2H), 1.37 (t, *J* = 7.0 Hz, 10H), 0.90 (t, *J* = 6.8 Hz, 3H). $^{13}C\{^{1}H\}$ NMR (101 MHz, $CDCl_3$) δ 63.4 (d, *J* = 5.9 Hz), 31.05-30.30 (m), 22.1, 16.0 (d, *J* = 7.3 Hz), 13.9. ^{31}P NMR (162 MHz, $CDCl_3$) δ 28.4. HRMS (ESI) m/z: calculated for $C_9H_{22}O_3PS$ $[M+H]^+$: 241.1022, found: 241.1024.

methyl 3-((diethoxyphosphoryl)thio)propanoate ***(3u)*** [13b] colorless oil (32.3 mg, 63% yield); ^{1}H NMR (400 MHz, $CDCl_3$) δ 4.17 (pd, *J* = 9.9, 5.1 Hz, 4H), 3.72 (s, 3H), 3.08 (dt, *J* = 16.4, 7.1 Hz, 2H), 2.77 (t, *J* = 7.1 Hz, 2H), 1.37 (t, *J* = 7.1 Hz, 6H). $^{13}C\{^{1}H\}$ NMR (101 MHz, $CDCl_3$) δ 171.6, 63.7 (d, *J* = 6.1 Hz), 51.9, 35.4 (d, *J* = 3.9 Hz), 25.6 (d, *J* = 4.1 Hz), 16.0 (d, *J* = 7.3 Hz).

ethyl 3-((diethoxyphosphoryl)thio)propanoate ***(3v)*** colorless oil (35.1 mg, 65% yield); ^{1}H NMR (400 MHz, $CDCl_3$) δ 4.30-4.03 (m, 6H), 3.08 (dt, *J* = 16.4, 7.1 Hz, 2H), 2.75 (t, *J* = 7.1 Hz, 2H), 1.37 (t, *J* = 7.0 Hz, 6H), 1.27 (t, *J* = 7.1 Hz, 3H). $^{13}C\{^{1}H\}$ NMR (101 MHz, $CDCl_3$) δ 171.2, 63.7 (d, *J* = 6.0 Hz), 60.8, 35.6 (d, *J* = 3.9 Hz), 25.7 (d, *J* = 4.1 Hz), 16.0 (d, *J* = 7.3 Hz), 14.2. ^{31}P NMR (162 MHz, $CDCl_3$) δ 27.2. HRMS (ESI) m/z: calculated for $C_9H_{20}O_5PS$ $[M+H]^+$: 271.0764, found: 271.0766.

S-(4-(tert-butyl)phenyl) O,O-diisopropyl phosphorothioate ***(3w)*** [13b] colorless oil (48.2 mg, 73% yield); ^{1}H NMR (400 MHz, $CDCl_3$) δ 7.44 (dd, *J* = 8.3, 1.7 Hz, 2H), 7.27 (d, *J* = 8.3 Hz, 2H), 4.69 (td, *J* = 12.4, 6.2 Hz, 2H), 1.26 (d, *J* = 6.2 Hz, 6H), 1.22 (s, 9H), 1.18 (d, *J* = 6.2 Hz, 6H). ^{13}C{^{1}H} NMR (101 MHz, $CDCl_3$) δ 152.1 (d, *J* = 3.0 Hz), 134.1 (d, *J* = 5.4 Hz), 126.3 (d, *J* = 2.1 Hz), 123.6 (d, *J* = 7.1 Hz), 73.2 (d, *J* = 6.8 Hz), 34.6, 31.2, 23.9 (d, *J* = 4.1 Hz), 23.5 (d, *J* = 5.7 Hz).

O,O-dibutyl S-(4-(tert-butyl)phenyl) phosphorothioate ***(3x)*** colorless oil (48 mg, 67% yield); ^{1}H NMR (400 MHz, $CDCl_3$) δ 7.41 (dd, *J* = 8.4, 1.8 Hz, 2H), 7.28 (d, *J* = 8.3 Hz, 2H), 4.12-3.95 (m, 4H), 1.64-1.48 (m, 4H), 1.33-1.19 (m, 13H), 0.82 (t, *J* = 7.4 Hz, 6H). ^{13}C{^{1}H} NMR (101 MHz, $CDCl_3$) δ 152.3 (d, *J* = 3.0 Hz), 134.3 (d, *J* = 5.2 Hz), 126.4 (d, *J* = 2.1 Hz), 123.0 (d, *J* = 7.1 Hz), 67.7 (d, *J* = 6.6 Hz), 34.7, 32.1 (d, *J* = 7.1 Hz), 31.2, 18.6, 13.5. ^{31}P NMR (162 MHz, $CDCl_3$) δ 23.4. HRMS (ESI) m/z: calculated for $C_{18}H_{32}O_3PS$ $[M+H]^+$: 359.1804, found: 359.1808.

S-(4-(tert-butyl)phenyl) diphenylphosphinothioate ***(3y)*** [12f] White solid (47.6 mg, 65% yield); ^{1}H NMR (400 MHz, $CDCl_3$) δ 7.91-7.76 (m, 4H), 7.56-7.48 (m, 2H), 7.44 (dt, *J* = 10.6, 5.3 Hz, 4H), 7.38-7.32 (m, 2H), 7.21 (d, *J* = 8.3 Hz, 2H), 1.24 (s, 9H). ^{13}C{^{1}H} NMR (101 MHz, $CDCl_3$) δ 152.3, 135.2 (d, *J* = 3.6 Hz), 133.3, 132.2 (d, *J* = 2.9 Hz), 131.7 (d, *J* = 10.2 Hz), 128.5 (d, *J* = 13.1 Hz), 126.3, 122.3, 34.6, 31.1.

S-(4-(tert-butyl)phenyl) O-ethyl phenylphosphonothioate ***(3z)*** [12f] colorless oil (50 mg, 75% yield); ^{1}H NMR (400 MHz, $CDCl_3$) δ 7.56 (dd, *J* = 13.5, 7.7 Hz, 2H), 7.40 (t, *J* = 7.3 Hz, 1H), 7.27 (dd, *J* = 11.7, 6.4 Hz, 2H), 7.13 (s, 4H), 4.27 (dd, *J* = 15.0, 7.4 Hz, 2H), 1.32 (t, *J* = 7.0 Hz, 3H), 1.18 (s, 9H). ^{13}C{^{1}H} NMR (101 MHz, $CDCl_3$) δ 152.4 (d, *J* = 3.0 Hz), 135.2 (d, *J* = 4.1 Hz), 132.4 (d, *J* = 2.9 Hz), 131.4 (d, *J* = 10.6 Hz), 130.9, 128.1 (d, *J* = 14.9 Hz), 126.2 (d, *J* = 2.1 Hz), 122.9 (d, *J* = 5.6 Hz), 62.4 (d, *J* = 7.0 Hz), 34.6, 31.2, 16.4 (d, *J* = 6.7 Hz).

S-benzyl O,O-diisopropyl phosphorothioate ***(3aa)*** [13b] colorless oil (35.7 mg, 62% yield); ^{1}H NMR (400 MHz, $CDCl_3$) δ 7.30 (ddd, *J* = 23.1, 14.1, 7.0 Hz, 5H), 4.69 (ddt, *J* = 12.4, 9.1, 6.2 Hz, 2H), 4.06 (d, *J* = 13.0 Hz, 2H), 1.33 (d, *J* = 6.2 Hz, 6H), 1.28 (d, *J* = 6.2 Hz, 6H). ^{13}C{^{1}H} NMR (101 MHz, $CDCl_3$) δ 137.5 (d, *J* = 6.2 Hz), 128.9, 128.7, 127.6, 72.7 (d, *J* = 6.3 Hz), 35.2 (d, *J* = 3.8 Hz), 23.8 (d, *J* = 4.1 Hz), 23.5 (d, *J* = 5.6 Hz).

S-benzyl O-ethyl phenylphosphonothioate ***(3ab)*** [12d] colorless oil (38 mg, 65% yield); ^{1}H NMR (400 MHz, $CDCl_3$) δ 7.83 (dd, *J* = 13.8, 7.3 Hz, 2H), 7.54 (t, *J* = 6.8 Hz, 1H), 7.45 (dd, *J* = 11.7, 7.3 Hz, 2H), 7.22 (s, 5H), 4.31-4.07 (m, 2H), 3.95 (dt, *J* = 23.8, 12.9 Hz, 2H), 1.34 (t, *J* = 7.0 Hz, 3H). ^{13}C{^{1}H} NMR (101 MHz, $CDCl_3$) δ 137.2 (d, *J* = 5.3 Hz), 133.3, 132.5 (d, *J* = 3.1 Hz), 131.8, 131.2 (d, *J* = 10.9 Hz), 128.9, 128.5 (d, *J* = 13.0 Hz), 127.4, 62.3 (d, *J* = 6.8 Hz), 34.5 (d, *J* = 2.6 Hz), 16.3 (d, *J* = 6.9 Hz).

O,O-diethyl S-(2-(ethylthio)ethyl) phosphorothioate ***(3ac)*** [13b] colorless oil (37.2 mg, 72% yield); ^{1}H NMR (400 MHz, $CDCl_3$) δ 4.27-4.09 (m, 4H), 3.09-2.97 (m, 2H), 2.84 (dd, *J* = 14.6, 6.0 Hz, 2H), 2.59 (dd, *J* = 14.7, 7.3 Hz, 2H), 1.37 (t, *J* = 7.0 Hz, 6H), 1.28 (t, *J* = 7.4 Hz, 3H). ^{13}C{^{1}H} NMR (101 MHz, $CDCl_3$) δ 63.7 (d, *J* = 6.1 Hz), 32.5 (d, *J* = 4.3 Hz), 30.7 (d, *J* = 3.7 Hz), 25.9, 16.1 (d, *J* = 7.2 Hz), 14.8.

S-(2-(dimethylamino)ethyl) O,O-diethyl phosphorothioate ***(3ad)*** [13b] colorless oil (33.3 mg, 69% yield); ^{1}H NMR (400 MHz, $CDCl_3$) δ 4.24-3.97 (m, 4H), 2.88 (dt, *J* = 13.9, 7.1 Hz, 2H), 2.53 (t, *J* = 7.0 Hz, 2H), 2.21 (s, 6H), 1.30 (t, *J* = 7.0 Hz, 6H). ^{13}C{^{1}H} NMR (101 MHz, $CDCl_3$) δ 63.6 (d, *J* = 6.1 Hz), 59.4 (d, *J* = 5.7 Hz), 45.1, 28.6 (d, *J* = 3.6 Hz), 16.1 (d, *J* = 7.2 Hz).

ASSOCIATED CONTENT

Supporting Information

The Supporting Information is available free of charge on the ACS Publications website General methods, extra information about the optimization of reaction conditions, ^{1}H NMR, ^{13}C NMR, ^{31}P NMR and HRMS spectra.

AUTHOR INFORMATION

Corresponding Author

* gyin@hust.edu.cn

Notes

The authors declare no competing financial interest.

ACKNOWLEDGMENT

This work was financially supported by the National Natural Science Foundation of China (No. 21573082) and the Graduates' Innovation Fund of Huazhong University of Science and Technology (No. 5003013019). The NMR and HRMS analyses were performed in the Analytical and Testing Center of Huazhong University of Science and Technology.

REFERENCES

(1) (a) Wu, Y.; Wang, J.; Mao, F.; Kwong, F. Y. Palladium-Catalyzed Cross-Dehydrogenative Functionalization of C(sp^2)-H Bonds. *Chem. Asian J.*, **2014**, *9*, 26-47. (b) Girard, S. A.; Knauber, T.; Li, C. J. The Cross-Dehydrogenative Coupling of C-H Bonds: A Versatile Strategy for C-C Bond Formations. *Angew. Chem. Int. Ed*., **2014**, *53*, 74-100. (c) Ruan, J.; Li, X.; Saidi, O.; Xiao, J. Oxygen and Base-Free Oxidative Heck Reactions of Arylboronic Acids with Olefins. *J. Am. Chem. Soc*., **2008**, *130*, 2424-2425. (d) Zhang, H.; Ferreira, E. M.; Stoltz, B. M. Pd-Catalyzed Cyclizations: Direct Oxidative Heck Cyclizations: Intramolecular Fujiwara-Moritani Arylations for The Synthesis of Functionalized Benzofurans and Dihydrobenzofurans. *Angew. Chem., Int.*

Ed., **2004**, *43*, 6144-6148. (e) Yeung, C. S.; Dong, V. M. Catalytic Dehydrogenative Cross-Coupling: Forming Carbon-Carbon Bonds by Oxidizing Two Carbon-Hydrogen Bonds. *Chem. Rev*. **2011**, *111*, 1215-1292. (f) Stankiewicz, A.; Seidl, P. R. *From C-H to C-C Bonds: Cross-Dehydrogenative-Coupling*. Royal Society of Chemistry, **2014**.

(2) (a) Chen, X.; Engle, K. M.; Wang, D. H.; Yu, J. Q. Palladium (II)-Catalyzed C-H Activation/C-C Cross-Coupling Reactions: Versatility and Practicality. *Angew. Chem., Int. Ed*., **2009**, *48*, 5094-5115. (b) Wei, Y.; Su, W. $Pd(OAc)_2$-Catalyzed Oxidative C-H/C-H Cross-coupling of Electron-Deficient Polyfluoroarenes with Simple Arenes. *J. Am. Chem. Soc*., **2010**, *132*, 16377-16379. (c) Stuart, D. R.; Fagnou, K. The Catalytic Cross-Coupling of Unactivated Arenes. *Science*, **2007**, *316*, 1172-1175.

(3) (a) Tang, R. Y.; Guo, X. K.; Xiang, J. N.; Li, J. H. Palladium-Catalyzed Synthesis of 3-Acylated Indoles Involving Oxidative Cross-Coupling of Indoles with α-Amino Carbonyl Compounds. *J. Org. Chem*., **2013**, *78*, 11163-11171. (b) Luo, S.; Luo, F. X.; Zhang, X. S.; Shi, Z. J. Synthesis of Dibenzopyranones through Palladium-Catalyzed Directed C-H Activation/Carbonylation of 2-Arylphenols. *Angew. Chem., Int. Ed*., **2013**, *52*, 10598-10601. (c) Ren, L.; Jiao, N. Pd/Cu-Cocatalyzed Aerobic Oxidative Carbonylative Homocoupling of Arylboronic Acids and CO: A Highly Selective Approach to Diaryl Ketones. *Chem. Asian J.*, **2014**, *9*, 2411-2414.

(4) (a) Momiyama, N.; Kanan, M. W.; Liu, D. R. Synthesis of Acyclic α, β-unsaturated Ketones via Pd (II)-Catalyzed Intermolecular Reaction of Alkynamides and Alkenes. *J. Am. Chem. Soc*., **2007**, *129*, 2230-2231. (b) Lee, J. M.; Ahn, D. S.; Jung, D. Y.; Lee, J.; Do, Y.; Kim, S. K.; Chang, S. Hydrogen-Bond-Directed Highly Stereoselective Synthesis of Z-enamides via Pd-Catalyzed

Oxidative Amidation of Conjugated Olefins. *J. Am. Chem. Soc*., **2006**, *128*, 12954-12962. (c) Dwight, T. A.; Rue, N. R.; Charyk, D.; Josselyn, R.; DeBoef, B. C-C Bond Formation via Double C-H Functionalization: Aerobic Oxidative Coupling as a Method for Synthesizing Heterocoupled Biaryls. *Org. Lett*., **2007**, *9*, 3137-3139. (d) Djakovitch, L.; Rouge, P. New Homogeneously and Heterogeneously [Pd/Cu]-Catalysed C3-Alkenylation of Free NH-Indoles. *J. Mol. Catal. A: Chem*., **2007**, *273*, 230-239.

(5) (a) McDonald, R. I.; Liu, G.; Stahl, S. S. Palladium (II)-Catalyzed Alkene Functionalization via Nucleopalladation: Stereochemical Pathways and Enantioselective Catalytic Applications. *Chem. Rev*., **2011**, *111*, 2981-3019. (b) Sigman, M. S.; Werner, E. W. Imparting Catalyst Control upon Classical Palladium-Catalyzed Alkenyl C–H Bond Functionalization Reactions. *Acc. Chem. Res*., **2012**, *45*, 874-884. (c) Kotov, V.; Scarborough, C. C.; Stahl, S. S. Palladium-Catalyzed Aerobic Oxidative Amination of Alkenes: Development of Intra-and Intermolecular Aza-Wacker Reactions. *Inorg. Chem*., **2007**, *46*, 1910-1923.

(6) (a) Sigman, M. S.; Jensen, D. R. Ligand-Modulated Palladium-Catalyzed Aerobic Alcohol Oxidations. *Acc. Chem. Res*., **2006**, *39*, 221-229. (b) Liang, P.; Xiong, H.; Guo, H.; Yin, G. Pd-Catalyzed C–H Bond Activation of Benzene in the CO_2-Expanded Solvent. *Catal. Commun*., **2010**, *11*, 560-562.

(7) (a) Yiu, S. M.; Wu, Z. B.; Mak, C. K.; Lau, T. C. $FeCl_3$-Activated Oxidation of Alkanes by $[Os(N)O_3]^-$. *J. Am. Chem. Soc*., **2004**, *126*, 14921-14929. (b) Lam, W. W.; Yiu, S. M.; Lee, J. M.; Yau, S. K.; Kwong, H. K.; Lau, T. C.; Liu. D.; Lin, Z. BF_3-Activated Oxidation of Alkanes by MnO_4. *J. Am. Chem. Soc*., **2006**, *128*, 2851-2858. (c) Miller, C. G.; Gordon-Wylie, S. W.; Horwitz, C. P.; Strazisar, S. A.; Peraino, D. K.; Clark, G. R.; Weintraub S. T.; Collins, T. J. A

Method for Driving O-atom Transfer: Secondary Ion Binding to a Tetraamide Macrocyclic Ligand. *J. Am. Chem. Soc.*, **1998**, *120*, 11540-11541. (d) Nam, W.; Lee, Y. M.; Fukuzumi, S. Tuning Reactivity and Mechanism in Oxidation Reactions by Mononuclear Nonheme Iron (IV)-Oxo Complexes. *Acc. Chem. Res*., **2014**, *47*, 1146-1154. (e) Park, J.; Morimoto, Y.; Lee, Y. M.; Nam, W.; Fukuzumi, S. Metal Ion Effect on The Switch of Mechanism from Direct Oxygen Transfer to Metal Ion-Coupled Electron Transfer in the Sulfoxidation of Thioanisoles by a Non-heme Iron (IV)-Oxo Complex. *J. Am. Chem. Soc*., **2011**, *133*, 5236-5239. (f) Park, J.; Morimoto, Y.; Lee, Y. M.; Nam, W.; Fukuzumi, S. Unified View of Oxidative C–H Bond Cleavage and Sulfoxidation by a Nonheme Iron (IV)-Oxo Complex via Lewis Acid-Promoted Electron Transfer. *Inorg. Chem*., **2014**, *53* (7), 3618-3628. (g) Yoon, H.; Lee, Y. M.; Wu, X.; Cho, K. B.; Sarangi, R.; Nam, W.; Fukuzumi, S. Enhanced Electron-Transfer Reactivity of Nonheme Manganese (IV)-Oxo Complexes by Binding Scandium Ions. *J. Am. Chem. Soc.*, **2013**, *135*, 9186-9194. (h) Leeladee, P.; Baglia, R. A.; Prokop, K. A.; Latifi, R.; de Visser, S. P.; Goldberg, D. P. Valence Tautomerism in a High-Valent Manganese-Oxo Porphyrinoid Complex Induced by a Lewis Acid. *J. Am. Chem. Soc*., **2012**, *134*, 10397-10400.

(8) (a) Dong, L.; Wang, Y.; Lv, Y.; Chen, Z.; Mei, F.; Xiong, H.; Yin, G. Lewis-Acid-Promoted Stoichiometric and Catalytic Oxidations by Manganese Complexes Having Cross-Bridged Cyclam Ligand: A Comprehensive Study. *Inorg. Chem*., **2013**, *52*, 5418-5427. (b) Chen, Z.; Yang, L.; Choe, C.; Lv, Z.; Yin, G. Non-redox Metal Ion Promoted Oxygen Transfer by a Non-heme Manganese Catalyst. *Chem. Comm*., **2015**, *51*, 1874-1877. (c) Zhang, Z.; Coats, K. L.; Chen, Z.; Hubin, T. J.; Yin, G. Influence of Calcium (II) and Chloride on the Oxidative Reactivity of a Manganese (II) Complex of a Cross-Bridged Cyclen Ligand. *Inorg. Chem*., **2014**, *53*,

11937-11947. (d) Choe, C.; Yang, L.; Lv, Z.; Mo, W.; Chen, Z.; Li, G.; Yin, G. Redox-inactive Metal Ions Promoted the Catalytic Reactivity of Non-heme Manganese Complexes Towards Oxygen Atom Transfer. *Dalton Trans*., **2015**, *44*, 9182-9192. (e) Zhang, J.; Wang, Y.; Luo, N.; Chen, Z.; Wu, K.; Yin, G. Redox Inactive Metal Ion Triggered N-dealkylation by an Iron Catalyst with Dioxygen Activation: A Lesson from Lipoxygenases. *Dalton Trans*., **2015**, *44*, 9847-9859. (f) Guo, H.; Chen, Z.; Mei, F.; Zhu, D.; Xiong, H.; Yin, G. Redox Inactive Metal Ion Promoted C-H Activation of Benzene to Phenol with Pd^{II}(bpym): Demonstrating New Strategies in Catalyst Designs. *Chem.- Asian J*., **2013**, *8*, 888-891. (g) Zhang, J.; Wei, W. J.; Lu, X.; Yang, H.; Chen, Z.; Liao, R. Z.; Yin, G. Nonredox Metal Ions Promoted Olefin Epoxidation by Iron (II) Complexes with H_2O_2: DFT Calculations Reveal Multiple Channels for Oxygen Transfer. *Inorg. Chem*., **2017**, *56*, 15138−15149.

(9) Qin, S.; Dong, L.; Chen, Z.; Zhang, S.; Yin, G. Non-redox Metal Ions can Promote Wacker-type Oxidations Even Better than Copper(II): A New Opportunity in Catalyst Design. *Dalton Trans*., **2015**, *44*, 17508-17515.

(10) (a) Senan, A. M.; Qin, S.; Zhang, S.; Lou, C.; Chen, Z.; Liao, R. Z.; Yin, G. Nonredox Metal-Ion-Accelerated Olefin Isomerization by Palladium (II) Catalysts: Density Functional Theory (DFT) Calculations Supporting the Experimental Data. *ACS Catal*., **2016**, *6*, 4144-4148. (b) Zhang, S.; Chen, Z.; Qin, S.; Lou, C.; Senan, A. M.; Liao, R. Z.; Yin, G. Non-redox Metal Ion Promoted Oxidative Coupling of Indoles with Olefins by the Palladium (II) Acetate Catalyst through Dioxygen Activation: Experimental Results with DFT Calculations. *Org. Biomol. Chem*., **2016**, *14*, 4146-4157. (c) Lou, C.; Qin, S.; Zhang, S.; Lv, Z.; Senan, A. M.; Chen, Z.; Yin, G. Non-Redox Metal Ions Promoted Oxidative Dehydrogenation of Saturated C-C Bond by Simple

$Pd(OAc)_2$ catalyst. *Catal. Commun*., **2017**, *90*, 5-9. (d) Zhang, S.; Xu, H.; Lou, C.; Senan, A. M.; Chen, Z.; Yin, G. Efficient Bimetallic Catalysis of Nitrile Hydration to Amides with a Simple $Pd(OAc)_2$/Lewis Acid Catalyst at Ambient Temperature. *Eur. J. Org. Chem.*, **2017**, *2017* 1870-1875. (e) Xue, J. W.; Zeng, M.; Hou, X.; Chen, Z.; Yin, G. Catalytic Oxidation of Alkynes into 1, 2-Diketone Derivatives by Using a Pd^{II}/Lewis-Acid Catalyst. *Asian J. Org. Chem*., **2018**, *7*, 212-219. (f) Senan, A. M.; Zhang, S.; Qin, S.; Chen, Z.; Yin, G. Transformation of Methyl Linoleate to its Conjugated Derivatives with Simple $Pd(OAc)_2$/Lewis Acid Catalyst. *J Am Oil Chem Soc*., **2017**, *94*, 1481-1489. (g) Senan, A. M.; Zhang, S.; Zeng, M.; Chen, Z.; Yin, G. Transformation of Unsaturated Fatty Acids/Esters to Corresponding Keto Fatty Acids/Esters by Aerobic Oxidation with Pd (II)/Lewis Acid Catalyst. *J. Agric. Food Chem*., **2017**, *65*, 6912-6918.

(11) (a) Quin L. D. A Guide to Organophosphorus Chemistry, *Wiley Interscience*, New York, 2000. (b) Murphy P. J. *Organophosphorus Reagents*, Oxford University Press, Oxford, UK, 2004. (c) Gallo M. A.; Lawryk N. J. Organic Phosphorus Pesticides. *The Handbook of Pesticide Toxicology*, Academic Press, San Diego, 1991. (d) Li, N. S.; Frederiksen, J. K.; Piccirilli, J. A. Synthesis, Properties, and Applications of Oligonucleotides Containing an RNA Dinucleotide Phosphorothiolate Linkage. *Acc. Chem. Res*., **2011**, *44*, 1257-1269. (e) Carta, P.; Puljic, N.; Robert, C.; Dhimane, A. L.; Fensterbank, L.; Lacôte, E.; Malacria, M. Generation of Phosphorus-Centered Radicals via Homolytic Substitution at Sulfur. *Org. Lett*., **2007**, *9*, 1061-1063. (f) Kumar, T. S.; Yang, T.; Mishra, S.; Cronin, C.; Chakraborty, S.; Shen, J. B.; Liang. B. T.; Jacobson, K. A. 5′-Phosphate and 5′-Phosphonate Ester Derivatives of (N)-methanocarba Adenosine with in Vivo Cardioprotective Activity. *J. Med. Chem*., **2013**, *56*, 902-914. (g) Cogoi, S.; Rapozzi, V.; Quadrifoglio, F.; Xodo, L. Anti-Gene Effect in Live Cells of AG Motif

Triplex-Forming Oligonucleotides Containing an Increasing Number of Phosphorothioate Linkages. *Biochemistry*, **2001**, *40*, 1135-1143.

(12) (a) Liu, Y. C.; Lee, C. F. N-Chlorosuccinimide-Promoted Synthesis of Thiophosphates from Thiols and Phosphonates under Mild Conditions. *Green Chem*., **2014**, *16*, 357-364. (b) Bai, J.; Cui, X.; Wang, H.; Wu, Y. Copper-Catalyzed Reductive Coupling of Aryl Sulfonyl Chlorides with H-Phosphonates Leading to S-aryl Phosphorothioates. *Chem. Commun*., **2014**, *50*, 8860-8863. (c) Li, S.; Chen, T.; Saga, Y.; Han, L. B. Chloroform-Based Atherton–Todd-type Reactions of Alcohols and Thiols with Secondary Phosphine Oxides Generating Phosphinothioates and Phosphinates. *RSC Adv*., **2015**, *5*, 71544-71546. (d) Wang, J.; Huang, X.; Ni, Z.; Wang, S.; Wu, J.; Pan, Y. TBPB-Promoted Metal-Free Synthesis of Thiophosphinate/Phosphonothioate by Direct P–S Bond Coupling. *Green Chem*., **2015**, *17*, 314-319. (e) Wang, J.; Huang, X.; Ni, Z.; Wang, S.; Pan, Y.; Wu, J. Peroxide Promoted Metal-Free Thiolation of Phosphites by Thiophenols/Disulfides. *Tetrahedron*, **2015**, *71*, 7853-7859. (f) Zhu, Y.; Chen, T.; Li, S.; Shimada, S.; Han, L. B. Efficient Pd-Catalyzed Dehydrogenative Coupling of P (O) H with RSH: A Precise Construction of P (O)–S Bonds. *J. Am. Chem. Soc*., **2016**, *138*, 5825-5828. (g) Sun, J. G.; Weng, W. Z.; Li, P.; Zhang, B. Dimethyl Sulfoxide as a Mild Oxidant in S-P (O) Bond Construction: Simple and Metal-Free Approaches to Phosphinothioates. *Green Chem*., **2017**, *19*, 1128-1133. (h) Zhang, X.; Wang, D.; An, D.; Han, B.; Song, X.; Li, L.; Zhang, G.; Wang, L. Cu(II)/Proline-Catalyzed Reductive Coupling of Sulfuryl Chloride and P (O)-H for P-S-C Bond Formation. *J. Org. Chem*., **2018**, *83*, 1532-1537. (i) Kaboudin, B.; Abedi, Y.; Kato, J.; Yokomatsu, T. Copper(I) Iodide Catalyzed Synthesis of Thiophosphates by Coupling of H-Phosphonates with Benzenethiols. *Synthesis*, **2013**, *45*, 2323-2327. (j) Huang, H.; Ash, J.;

Kang, J. Y. Base-Controlled Fe(Pc)-Catalyzed Aerobic Oxidation of Thiols for the Synthesis of S–S and S–P(O) Bonds. *Org. Biomol. Chem.*, **2018**, *16*, 4236-4242.

(13) (a) Sun, J. G.; Yang, H.; Li, P.; Zhang, B. Metal-Free Visible-Light-Mediated Oxidative Cross-Coupling of Thiols with P (O) H Compounds Using Air as the Oxidant. *Org. Lett.*, **2016**, *18*, 5114-5117. (b) Song, S.; Zhang, Y.; Yeerlan, A.; Zhu, B.; Liu, J.; Jiao, N. Cs_2CO_3-Catalyzed Aerobic Oxidative Cross-Dehydrogenative Coupling of Thiols with Phosphonates and Arenes. *Angew. Chem. Int. Ed.*, **2017**, *56*, 2487-2491. (c) He, W.; Hou, X.; Li, X.; Song, L.; Yu, Q.; Wang, Z. Synthesis of P (O)-S Organophosphorus Compounds by Dehydrogenative Coupling Reaction of P (O) H Compounds with Aryl Thiols in the Presence of Base and Air. *Tetrahedron*, **2017**, *73*, 3133-3138.

(14) (a) Xiao, W. J.; Alper, H. First Examples of Enantioselective Palladium-Catalyzed Thiocarbonylation of Prochiral 1, 3-Conjugated Dienes with Thiols and Carbon Monoxide: Efficient Synthesis of Optically Active β, γ-Unsaturated Thiol Esters. *J. Org. Chem.*, **2001**, *66*, 6229-6233. (b) Purohit, V. B.; Karad, S. C.; Patel, K. H.; Raval, D. K. Palladium N-Heterocyclic Carbene Catalyzed Regioselective Thiolation of 1-Aryl-3-methyl-1H-pyrazol-5 (4H)-ones Using Aryl Thiols. *Tetrahedron*, **2016**, *72*, 1114-1119. (c) Jin, L.; Wang, J.; Dong, G. Palladium-Catalyzed γ-C (sp^3)-H Arylation of Thiols by a Detachable Protecting/Directing Group. *Angew. Chem. Int. Ed.*, **2018**, *57*, 12352-12355.

(15) (a) Tucci, G. C.; Holm, R. H. Nickel-Mediated Formation of Thio Esters from Bound Methyl, Thiols, and Carbon Monoxide: A Possible Reaction Pathway of Acetyl-Coenzyme A Synthase Activity in Nickel-Containing Carbon Monoxide Dehydrogenases. *J. Am. Chem. Soc.*, **1995**, *117*, 6489-6496. (b) Rakass, S.; Oudghiri-Hassani, H.; Abatzoglou, N.; Rowntree, P. A Study of the

Surface Properties and Steam Reforming Catalytic Activity of Nickel Powders Impregnated by N-Alkanethiols. *J. Power Sources*, **2006**, *162*, 579-588. (c) Pelmenschikov, V.; Siegbahn, P. E. Nickel Superoxide Dismutase Reaction Mechanism Studied by Hybrid Density Functional Methods. *J. Am. Chem. Soc.*, **2006**, *128*, 7466-7475. (d) Ghorbani-Choghamarani, A.; Tahmasbi, B.; Arghand, F.; Faryadi, S. Nickel Schiff-Base Complexes Immobilized on Bboehmite Nanoparticles and their Application in the Oxidation of Sulfides and Oxidative Coupling of Thiols as Novel and Reusable Nano Organometal catalysts. *RSC Adv.*, **2015**, *5*, 92174-92183.

(16) (a) Zimdars, J.; Bredol, M. On the Influence of Coordinating Solvents on the Reduction of Selenium for the Phosphine-Free Synthesis of Metal Selenide Nanoparticles. *New J. Chem.,* **2016**, *40*, 1137-1142. (b) Yang, Y.; Liu, W.; Wang, N.; Wang, H.; Song Z.; Li, W. Effect of Organic Solvent and Brønsted Acid on 5-Hydroxymethylfurfural Preparation from Glucose over $CrCl_3$. *RSC Adv*., **2015**, *5*, 27805–27813. (c) Niederberger, M.; Garnweitner, G. Organic Reaction Pathways in the Nonaqueous Synthesis of Metal Oxide Nanoparticles. *Chem. Eur. J.* **2006**, *12*, 7282-7302. (d) Zhao, G. J.; Han, K. L. Hydrogen Bonding in the Electronic Excited State. *Acc. Chem. Res.*, **2012**, *45*, 404-413.

(17) (a) Chen, Y.; Yao, J.; Wang, W. X.; Gao, T. C.; Yang, X.; Zhang, A. F. Effect of Epoxiconazole on Rice Blast and Rice Grain Yield in China., *Eur. J. Plant Pathol*, **2013**, *135*, 675-682. (b) Amin, U.; Akhtar, N. Effect of Fungicides on Nitrate Uptake and Assimilation in Aspergillusnidulans. *The J. Anim. Plant Sci.*, **2017**, *27*, 550-558.

(18) (a) Uesugi, Y.; Tomizawa, C. Metabolism of S-benzyl O-ethyl Phenylphosphonothioate (Inezin®) by Mycelial Cells of Pyricularia Oryzae. *Agric. Biol. Chem*., **1971**, *36*, 313-317. (b) Shabana, R. Studies on Organophosphorus Compounds. Part VI† the Reaction of Alkoxides with

2, 4-Bis (4-methoxyphenyl)-1, 3, 2, 4-dithiadiphosphetane 2, 4-disulfide (LR). A New Approach for Thio-inezin. *Phosphorus and Sulfur*, **1987**, *29*, 293-296.

(19) (a) Cowan Jr, C. B.; Davis, J. W.; Parencia Jr, C. R. Field Experiments against Several Late-Season Cotton Insects in 1959. *J. Econ. Entomol.*, **1960**, *53*, 747-749. (b) Cooke, B. K.; Herrington, P. J.; Jones, K. G.; Morgan, N. G. Pest and Disease Control on Intensive Apple Trees by Overhead Mobile Spraying. *Pestic. Sci*., **1975**, *6*, 571-579.

(20) (a) B'Ann, T. G.; Hennes, E. A.; Seeman, J. L.; Tian, B.; Kaufman, P. L. H-7 Effect on Outflow Facility after Trabecular Obstruction following Long-term Echothiophate Treatment in Monkeys. *Invest. Ophthalmol. Vis. Sci*., **2004**, *45*, 2732-2736. (b) Tammelin, L. E. Dialkoxyphosphorylthiocholines, Alkoxy-methylphosphorylthiocholines and Analogous Choline Esters-syntheses, pka of Tertiary Homologues and Cholinesterase Inhibition. *Acta Chem. Scand.*, **1957**, *11*, 1340-1349.

(21) (a) Zdilla, M. J.; Dexheimer, J. L.; Abu-Omar, M. M. Hydrogen Atom Transfer Reactions of Imido Manganese(V) Corrole: One Reaction with Two Mechanistic Pathways. *J. Am. Chem. Soc.*, **2007**, *129*, 11505-11511. (b) Parsell, T. H.; Yang, M.-Y.; Borovik, A. S. C-H Bond Cleavage with Reductants: Re-Investigating the Reactivity of Monomeric $Mn^{III/IV}$-Oxo Complexes and the Role of Oxo Ligand Basicity. *J. Am. Chem. Soc.*, **2009**, *131*, 2762-2763. (c) Fukuzumi, S.; Kotani, H.; Suenobu, T.; Hong, S.; Lee, Y.-M.; Nam, W. Contrasting Effects of Axial Ligands on Electron-Transfer Versus Proton-Coupled Electron-Transfer Reactions of Nonheme Oxoiron(IV) Complexes. *Chem. Eur. J.*, **2010**, *16*, 354-361. (d) Wang, Y.; Shi, S.; Wang, H.; Zhu, D.; Yin, G. Kinetics of Hydrogen Abstraction by Active Metal Hydroxo and Oxo Intermediates: Revealing their Unexpected Similarities in the Transition State. *Chem. Commun.*, **2012**, *48*, 7832-7834.

(22) (a) Hosokawa, T.; Nomura, T.; Murahashi, S. I. Palladium-Copper-DMF Complexes Involved in the Oxidation of Alkenes. *J. Organomet. Chem*., **1998**, *551*, 387-389. (b) Kozitsyna, N. Y.; Nefedov, S. E.; Dolgushin, F. M.; Cherkashina, N. V.; Vargaftik, M. N.; Moiseev, I. I. Heterodimetallic Pd^{II}-based Carboxylate-Bridged Complexes: Synthesis and Structure of Single-Crystalline Pd^{II}–M (M= Mn^{II}, Co^{II}, Ni^{II}, Cu^{II}, Zn^{II}, Nd^{III}, Eu^{III}, Ce^{IV}) Acetates. *Inorg. Chim. Acta.*, **2006**, *359*, 2072-2086. (c) Akhmadullina, N. S.; Cherkashina, N. V.; Kozitsyna, N. Y.; Gekhman, A. E.; Vargaftik, M. N. Unexpected Participation of Nucleophiles in the Reaction of Palladium (II) Acetate with Divalent 3d Metals. *Kinet. Catal*., **2009**, *50*, 396-400. (d) Huang, G. H.; Li, J. M.; Huang, J. J.; Lin, J. D.; Chuang, G. J. Cooperative Effect of Two Metals: $CoPd(OAc)_4$-Catalyzed C-H Amination and Aziridination. *Chem. Eur. J*., **2014**, *20*, 5240-5243.

(23) (a) Liang, X.; Wu, C.; Zheng, Z.; Walsh, P. J. Nickel-Catalyzed Oxidative Coupling Reaction of Phenyl Benzyl Sulfoxides. *Organometallics*, **2018**, *37*, 3132-3141. (b) Yin, W.; He, C.; Chen, M.; Zhang, H.; Lei, A. Nickel-Catalyzed Oxidative Coupling Reactions of Two Different Terminal Alkynes Using O_2 as the Oxidant at Room Temperature: Facile Syntheses of Unsymmetric 1,3-Diynes. *Org. Lett.*, **2009**, *11*, 709-712.

(24) (a) Zeng, L.; Miller, E. W.; Pralle, A.; Isacoff, E. Y.; Chang, C. J. A Selective Turn-On Fluorescent Sensor for Imaging Copper in Living Cells. *J. Am. Chem. Soc.*, **2006**, *128*, 10-11. (b) Hao, J.; Kos, P.; Zhou, K.; Miller, J. B.; Xue, L.; Yan, Y.; Xiong, H.; Elkassih, S.; Siegwart, D. J. Rapid Synthesis of a Lipocationic Polyester Library via Ring-Opening Polymerization of Functional Valerolactones for Efficacious siRNA Delivery. *J. Am. Chem. Soc.*, **2015**, *137*, 9206-9209.